Dynamos and Reconnection in Laboratory and Astrophysical Plasmas

Fatima Ebrahimi

Princeton Plasma Physics Laboratory and Dept. of Astrophysical Sciences,
Princeton University

2017 PPPL Summer SULI Thursday Seminar
July 13, 2017

Magnetic fields are observed to exist essentially everywhere in the universe

Galactic, geo, solar magnetic field

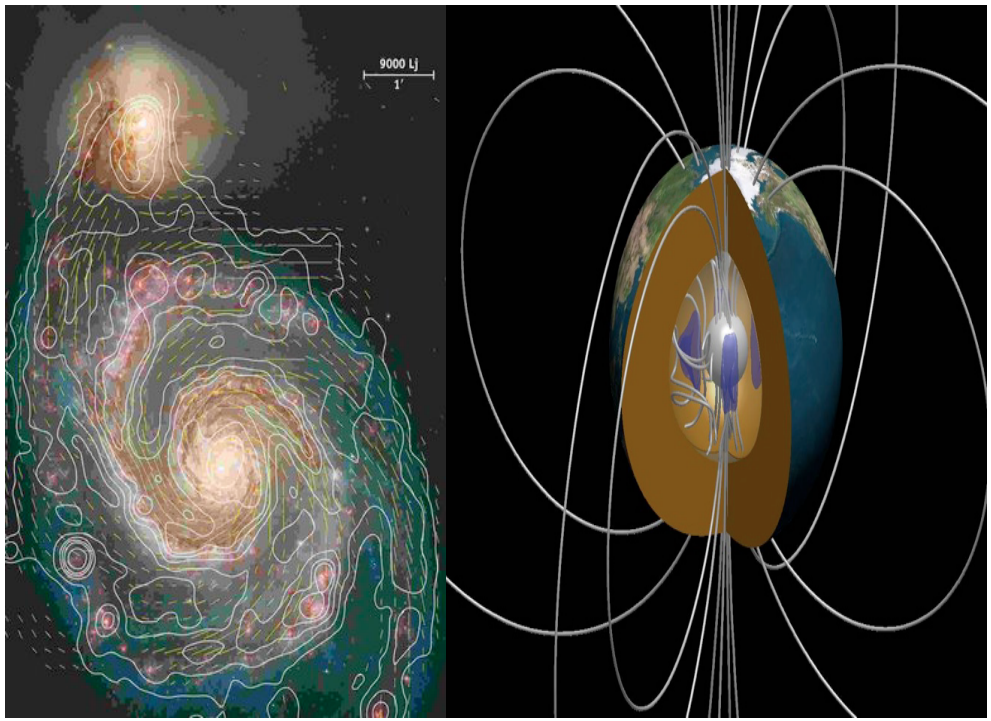

(Loading sunexplosion.mp4)

PPPL PRINCETON UNIVERSITY

Why is the universe magnetized?

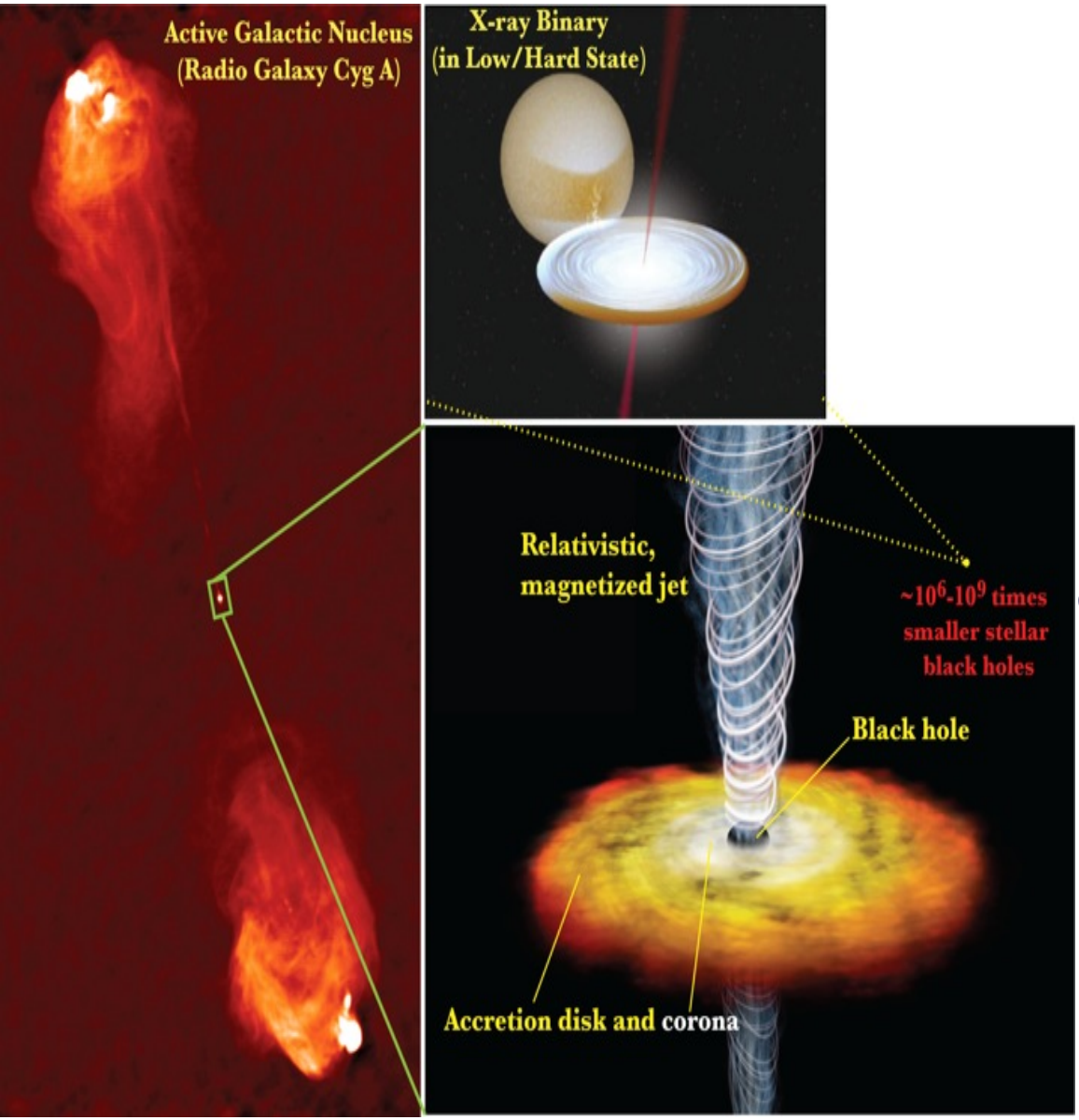

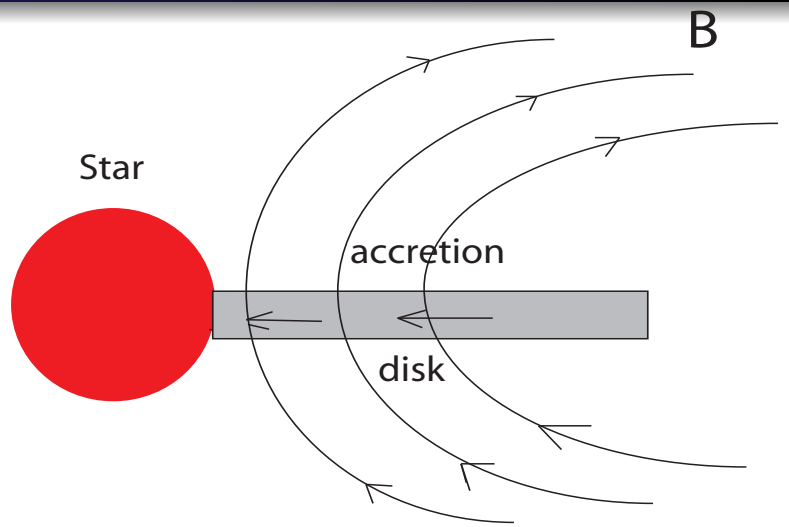

- Magnetic field is required to cause accretion, the collimation of jets and star formation.

PPPL PRINCETON UNIVERSITY

Self-organized plasmas are common throughout the universe

Examples of self-organized plasmas include

Flow-dominated: astrophysical disks

Magnetically-dominated: surface of stars (disk and stars coronas).

A disk-corona model

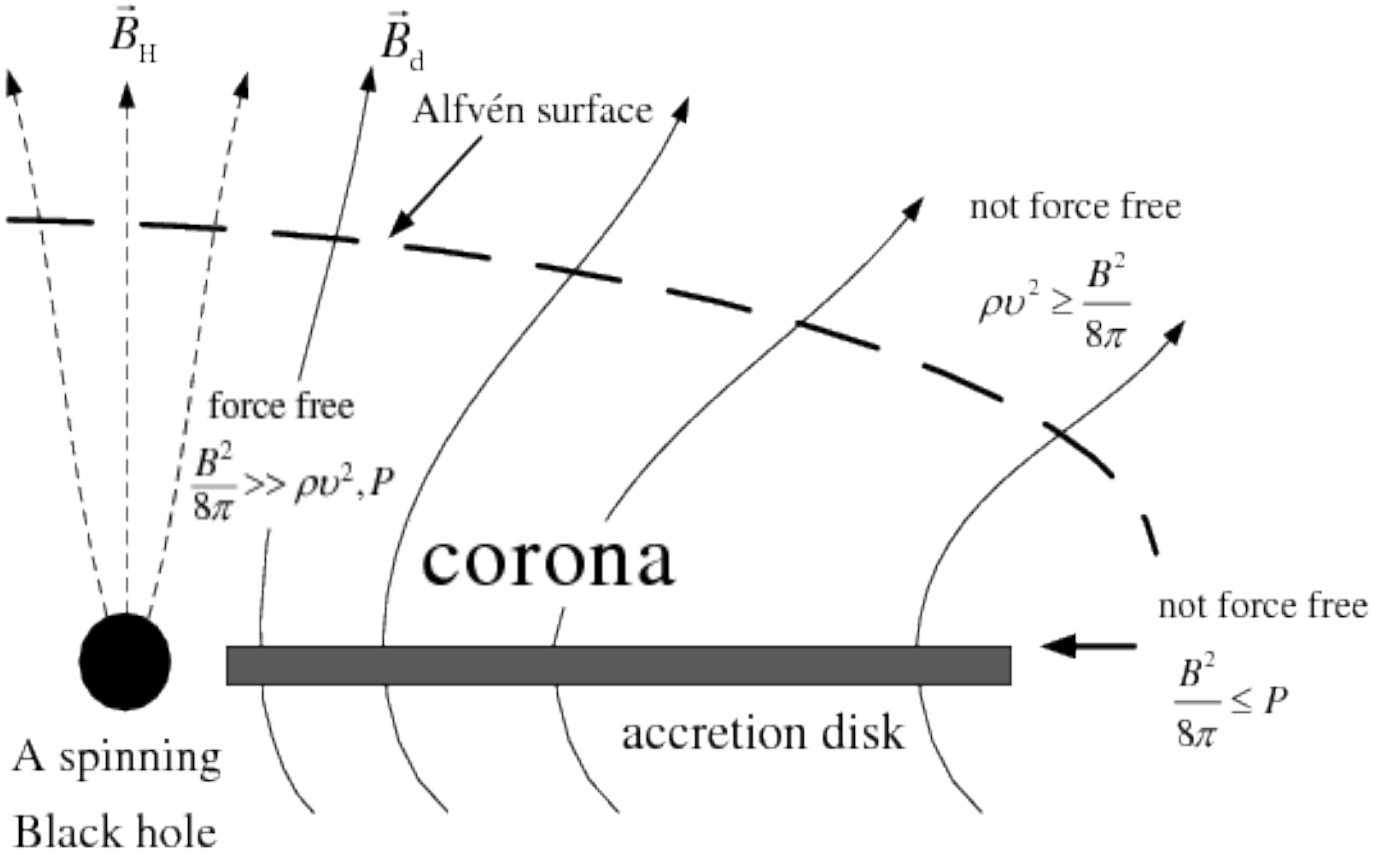

from Wang et al. RAA

What do we know about magnetic fields?

- Energy and flux are the most familiar global quantities of magnetic fields. How about the topological property?

Magnetic helicity, a topological property, measures the knottedness and the twistedness of magnetic fields

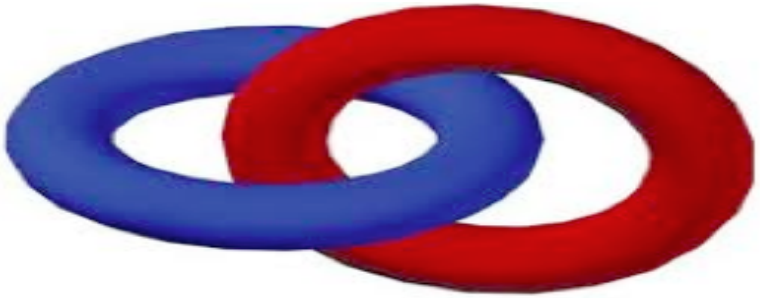

$$K = \int A \cdot B dV = 2\,\phi\ \phi$$

$$B d\mathbf{v}_1 = B \cdot \hat{n} ds_1 dl_1 = \Phi_1 dl_1$$

$$K_1 = \int \mathbf{A} \cdot \mathbf{B} d\mathbf{v}_l$$
$$= \Phi_1 \int \mathbf{A} \cdot dl_1 = \Phi_1 \Phi_2$$

Two interlinked flux tubes $\longrightarrow$

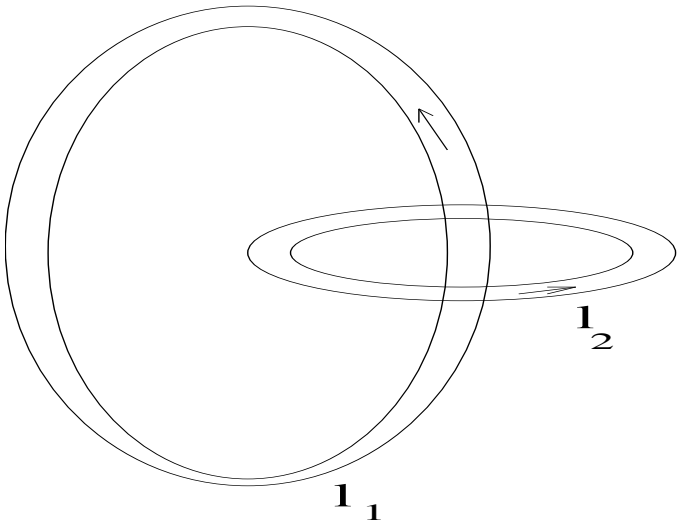

It can be shown that magnetic helicity is a rugged invariant

PPPL PRINCETON UNIVERSITY

Generation of magnetic field - energy and flux

Dynamo converts fluid kinetic energy into magnetic energy:

$$\rho V^2 \Rightarrow B^2/2\mu_0$$

- "Large-scale dynamo"– the generation of large-scale field accompanied by the generation of total magnetic flux.
- "Small-scale dynamo" – sustainment of magnetic energy due to magnetic fluctuations in a turbulent state with a small amount of flux.

Signatures of dynamo: production of magnetic energy, flux and helicity out of no, or seed, field

PPPL PRINCETON UNIVERSITY

Generation of magnetic field - energy and flux

Dynamo converts fluid kinetic energy into magnetic energy:

$$\rho V^2 \Rightarrow B^2/2\mu_0$$

- "Large-scale dynamo"– the generation of large-scale field accompanied by the generation of total magnetic flux.
- "Small-scale dynamo" – sustainment of magnetic energy due to magnetic fluctuations in a turbulent state with a small amount of flux.

Signatures of dynamo: production of magnetic energy, flux and helicity out of no, or seed, field

PPPL PRINCETON UNIVERSITY

- Can large-scale magnetic fields be generated through complex flows of plasmas (MHD dynamo)?

PPPL PRINCETON UNIVERSITY

How could a large-scale field grow?

Consider: mean seed field + differential rotation

B_0 and $V_\phi(z)$

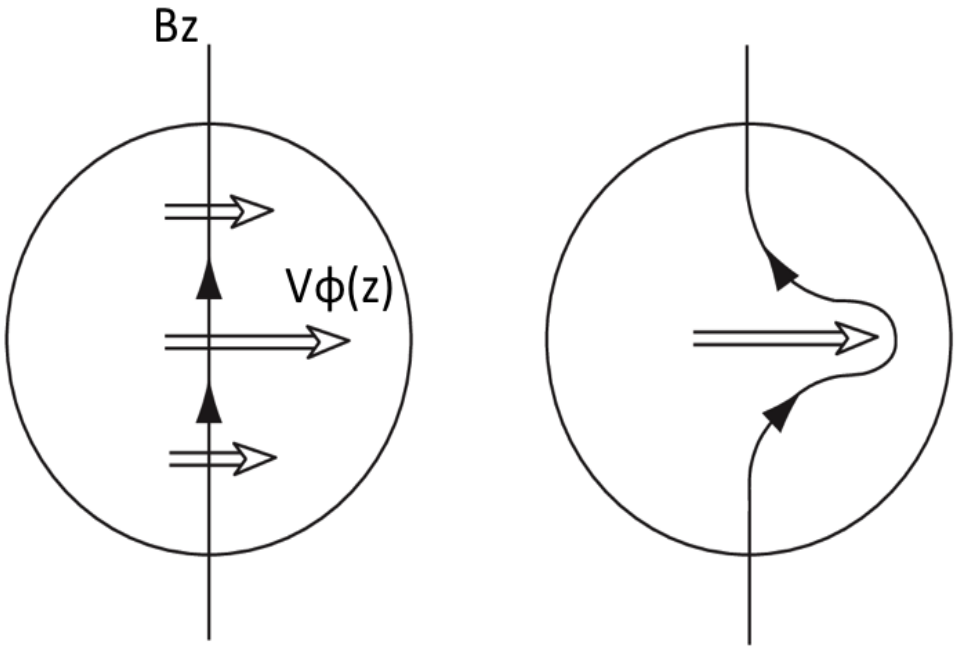

The Omega-effect:

Conversion of poloidal field to toroidal field by differential rotation (shear) of toroidal flows – (shear of the mean field by differential rotation)

Could a large-scale field grow out of turbulence?

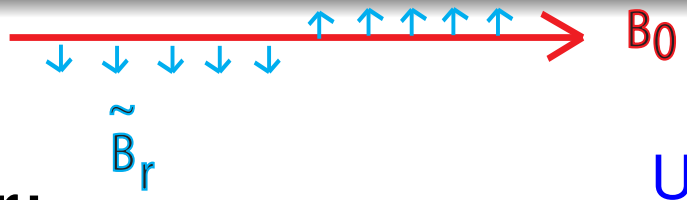

Consider:

$$V = < V > + \tilde{V}$$
$$B = < B > + \tilde{B}$$

large-scale small-scale

- fluctuations : $\tilde{\mathbf{B}}_{mn}(\mathbf{r}) = \tilde{\mathbf{B}}_{mn}(r)e^{i(m\phi - nz + \delta)} + \text{c.c}$
- $<>$, or overbars $\rightarrow$ azimuthally and axially averaged - surface-averaged $\int d\phi dz$
- $< \tilde{B} > = < \tilde{V} >= 0$

Unstratified Keplerian cylinder

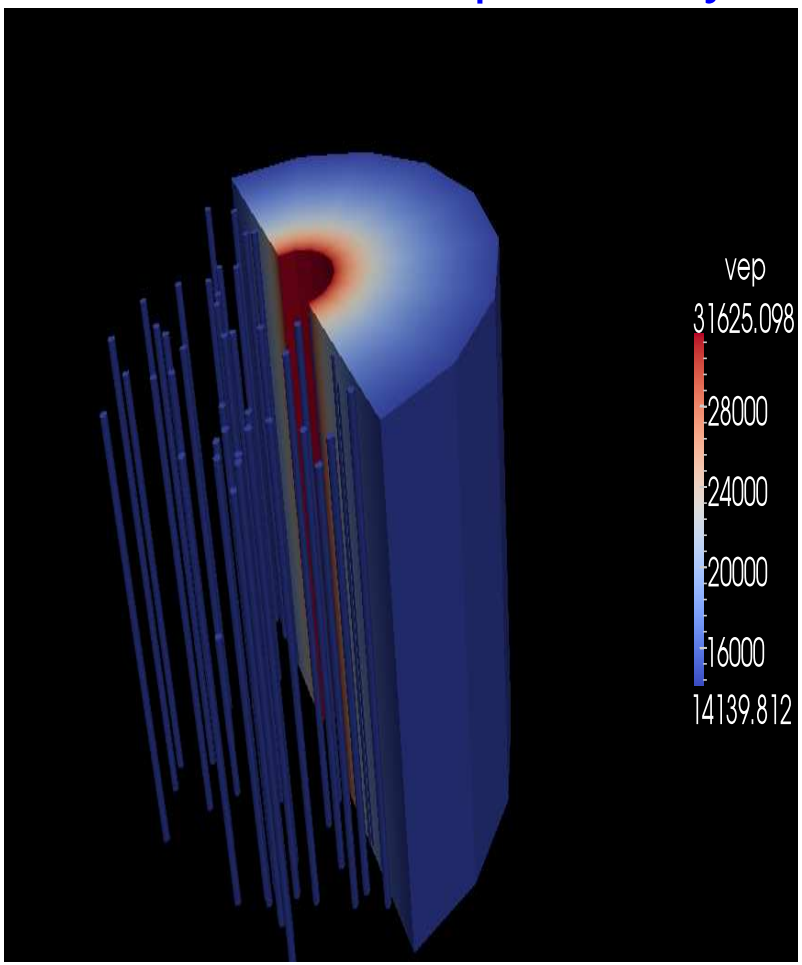

PPPL PRINCETON UNIVERSITY

Magnetic field interacts with the velocity field of the fluid through the induction equation

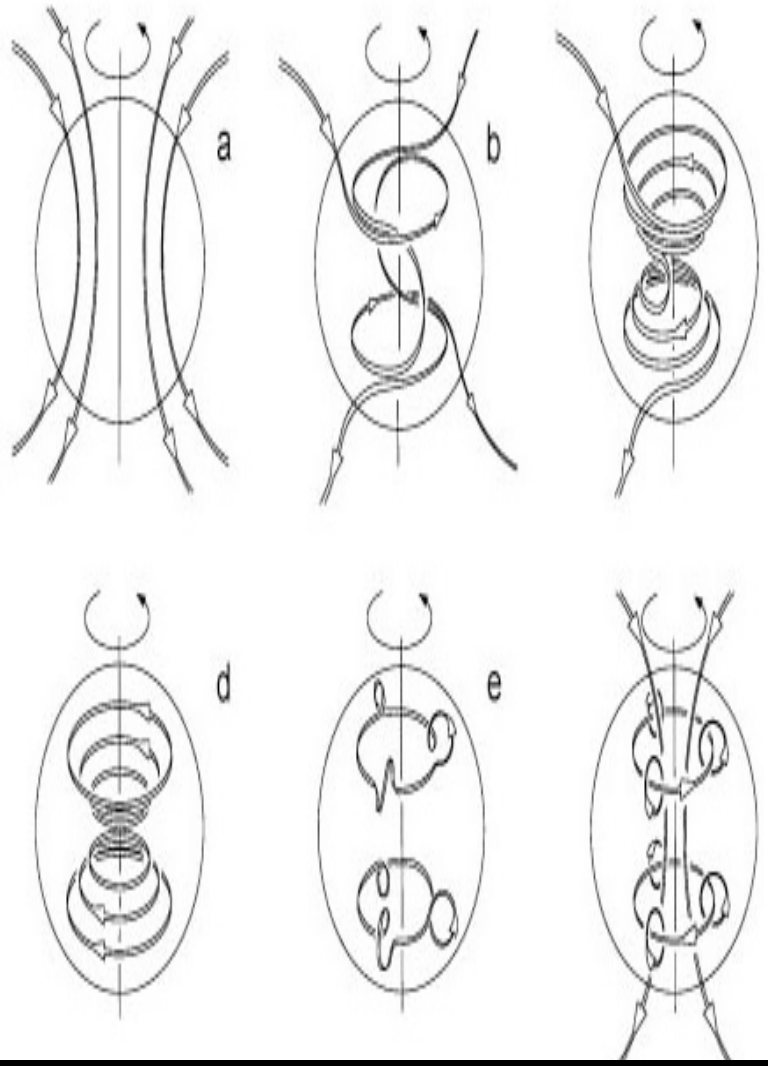

Magnetic field generation

$$\frac{\partial < \mathbf{B} >}{\partial t} = -\nabla \times < \mathbf{E} >$$

through fluid motions

$$< \mathbf{E} > = \underbrace{- < V > \times < B >}$$

Large-scale

through correlated fluctuations

$$< \mathbf{E} > = \underbrace{- < \tilde{V} \times \tilde{B} >}$$

Large-scale

Possible candidates for large-scale field generation

The Ω and α effects.

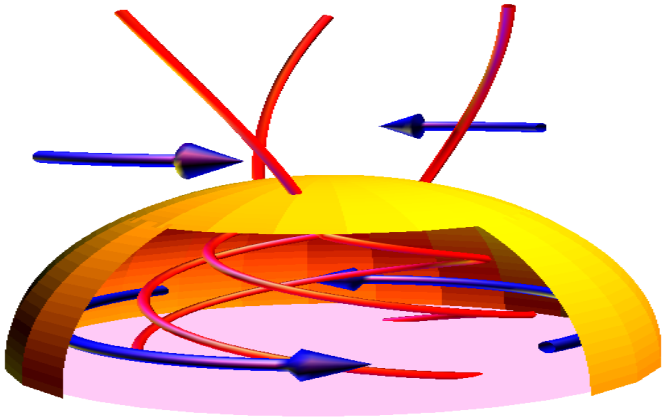

from Berger 99

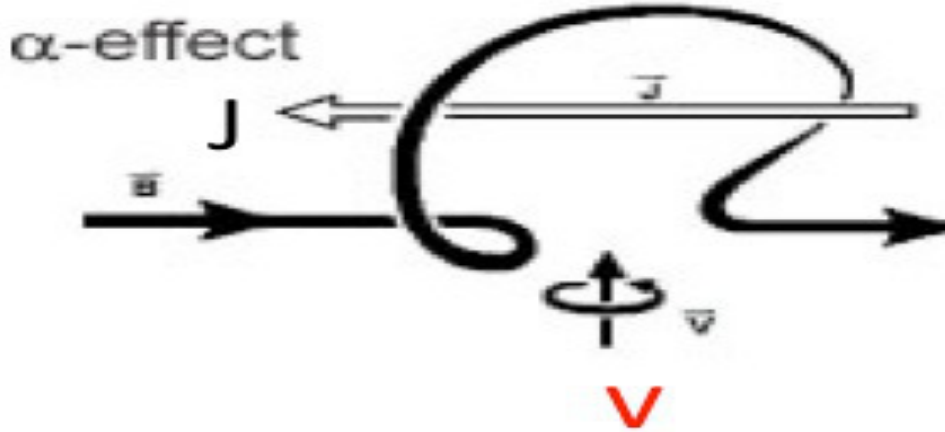

Differential rotation provides a strong source of helicity injection and field growth $\frac{\partial \overline{\mathbf{B}}}{\partial t} \propto \overline{\mathbf{B}}_0 \frac{d}{dz}\overline{\mathbf{V}}(z)$.

$\overline{\mathcal{E}}_{emf} \approx < \widetilde{V} \times \widetilde{B} >$

The electromotive force (EMF) from correlated velocity and magnetic field fluctuations

$$\frac{\partial \overline{\mathbf{B}}}{\partial t} = \nabla \times \left(\overline{\mathbf{V}} \times \overline{\mathbf{B}} + \overline{\mathcal{E}}_{emf} - \eta \nabla \times \overline{\mathbf{B}} \right)$$

PPPL PRINCETON UNIVERSITY

Evidence for large-scale magnetic field growth

Beyond stellar and galactic contexts, evidence for large-scale field growth is seen in

- magnetically dominated laboratory plasmas [Ji et al. 1995; Cothran et al. 2009]
- local and global simulations [Brandenburg et al. 1995; Ebrahimi et al. 2009; Lesur & Ogilvie 2010; Gressel 2010; Davis et al. 2010; Simon et al. 2011; Guan & Gammie 2011; Sorathia et al. 2012; Rincon et al 2007; Vishniac 2009; Ebrahimi & Bhattacharjee 2014, Squire & Bhattacharjee 2015; Suzuki & Inutsuka 2014; Ebrahimi & Blackman 2016; Bhat et al. 2016,] of the magnetorotational instability (MRI) [Velikhov 1959; Balbus & Hawley 1991]

PPPL PRINCETON UNIVERSITY

Flow-driven Magnetorotational Instability (MRI) turbulence in disk is an example of dynamo field generation

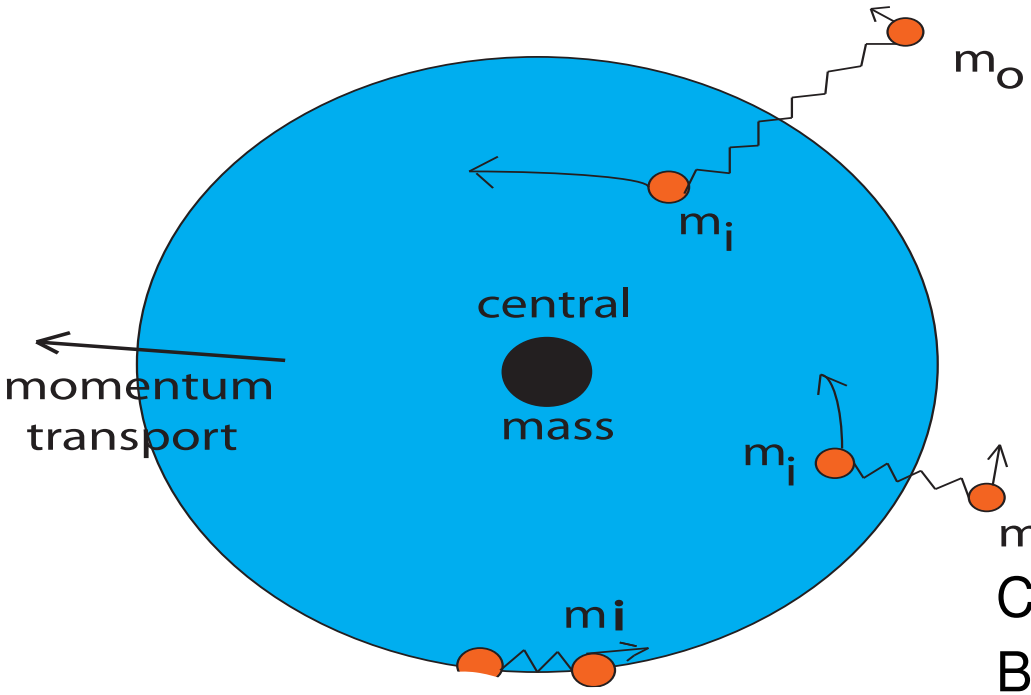

- MRI unstable if

$$(K \cdot V_A)^2 < -d\Omega^2/dln(r)$$

- Weak magnetic field causes MRI to grow

Velikhov(1959)
Chandrasekhar(1960)
Balbus and Hawley (1991)

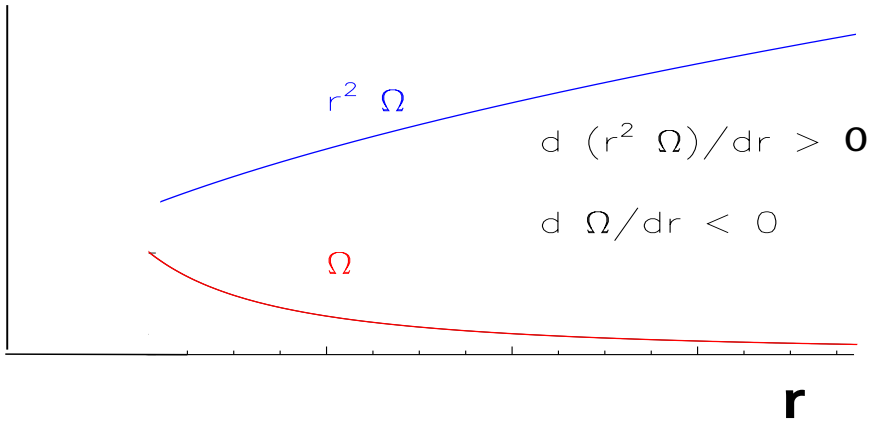

Two fluid elements rotate on different circular orbits and are connected by a spring (a magnetic field line in accretion disks)

PPPL PRINCETON UNIVERSITY

Evidence for large-scale field growth in local simulations of MRI

y-z averaged

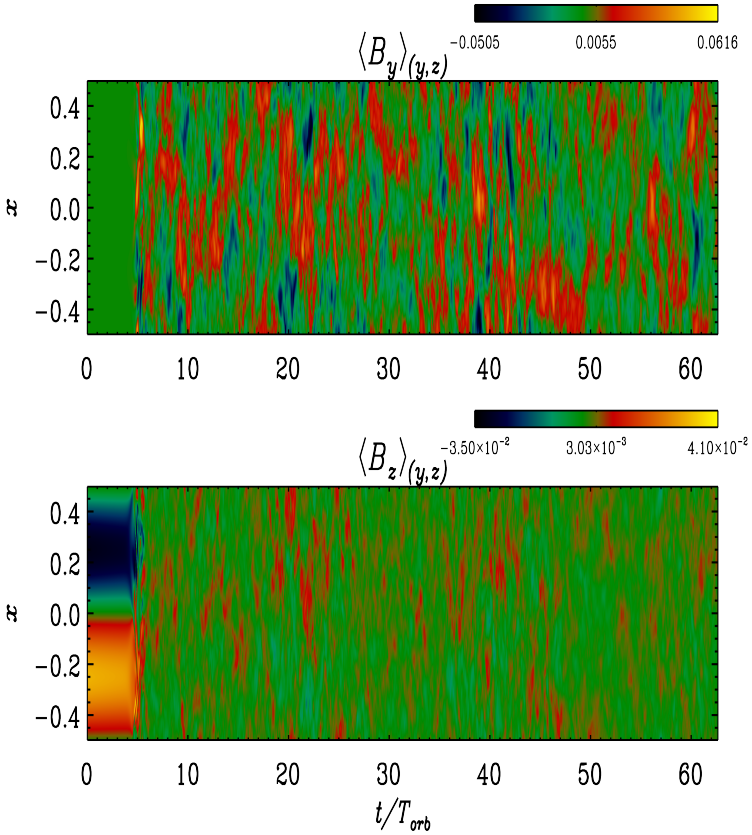

x-y averaged

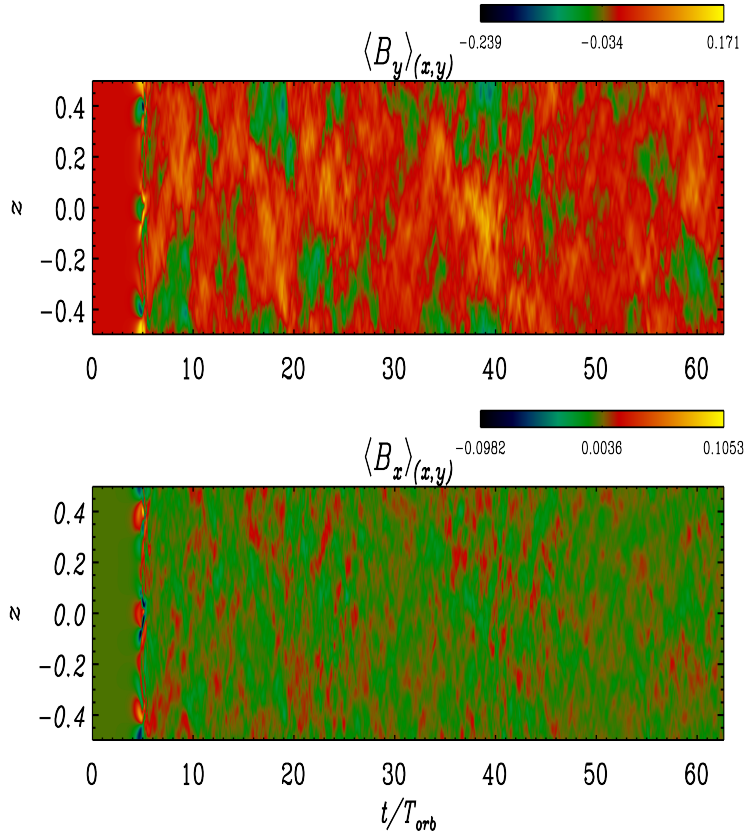

The yz averaged field here matches with that generated in global simulation of Ebrahimi and Blackman (2016).

Bhat, Ebrahimi & Blackman, MNRAS, 2016

PPPL PRINCETON UNIVERSITY

Large-scale toroidal field generated in unstratified simulations.
(averaged over vertical and toroidal directions in zero net-flux simulations)

3-D with all the Fourier modes

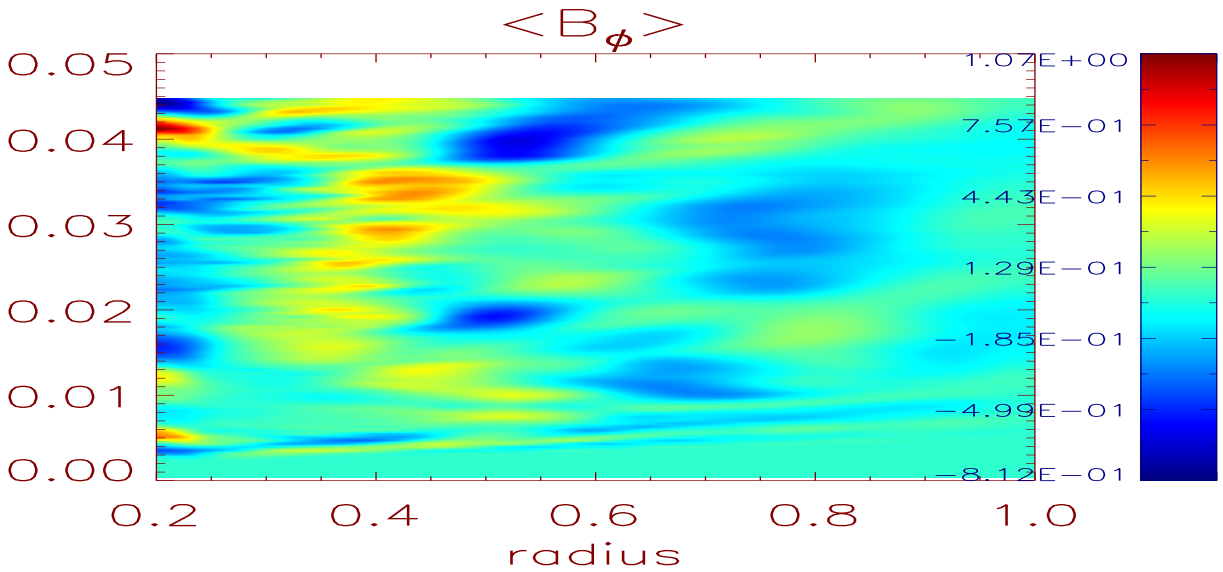

Single m=1 mode

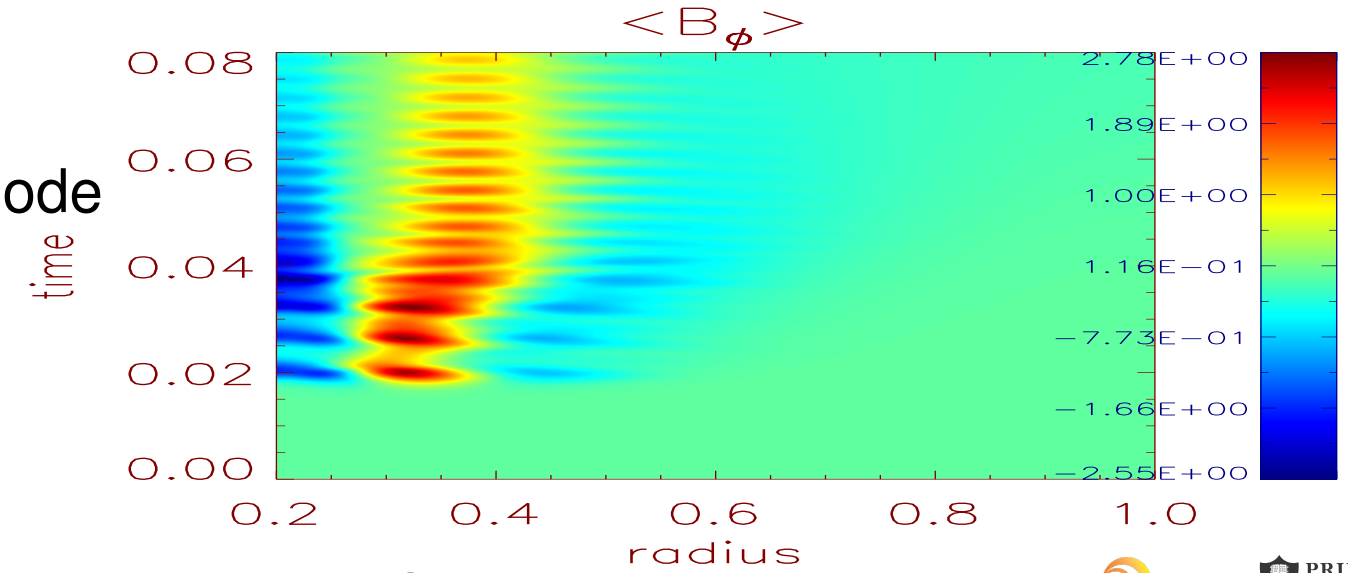

Ebrahimi& Blackman MNRAS 2016

PPPL PRINCETON UNIVERSITY

In 2-D, there is no generation of toroidal field or mean helicity

2-D simulations

F. Ebrahimi et al. ApJ. 2009

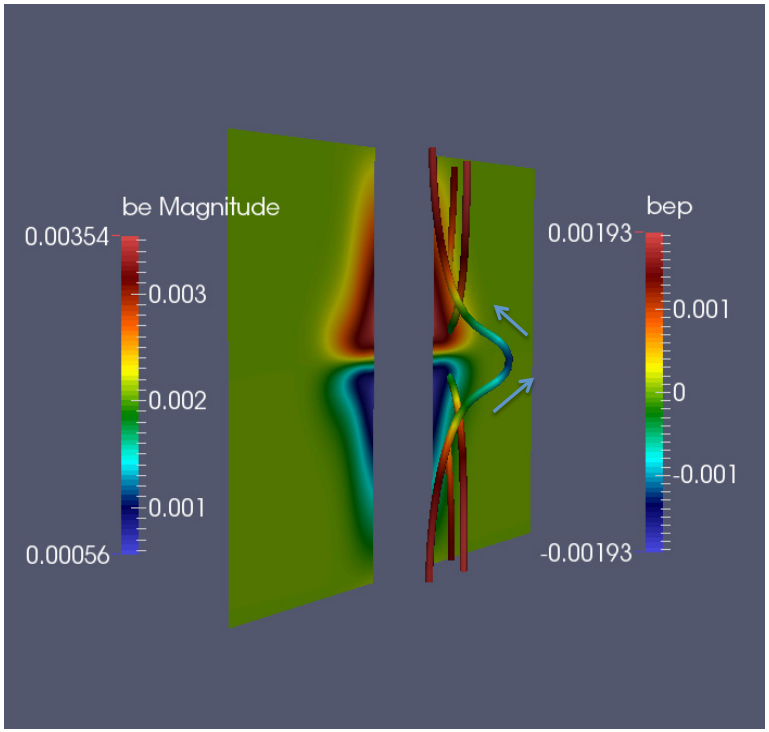

Top view

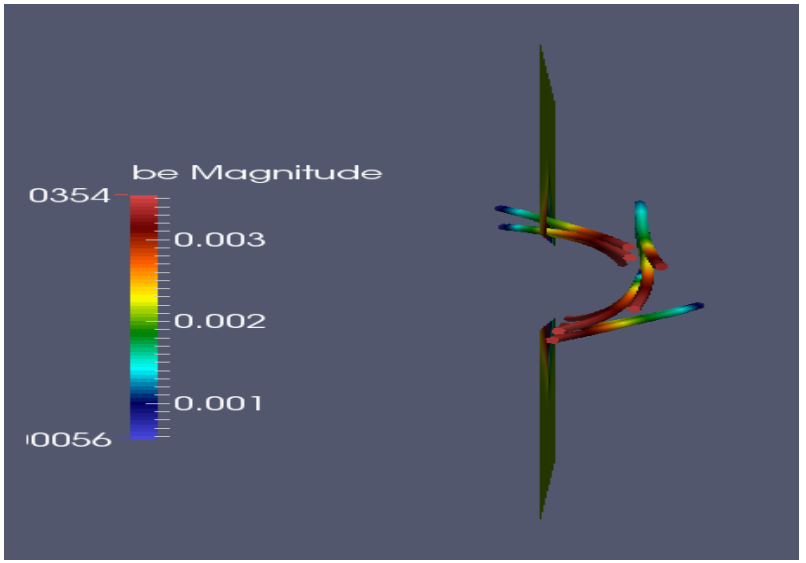

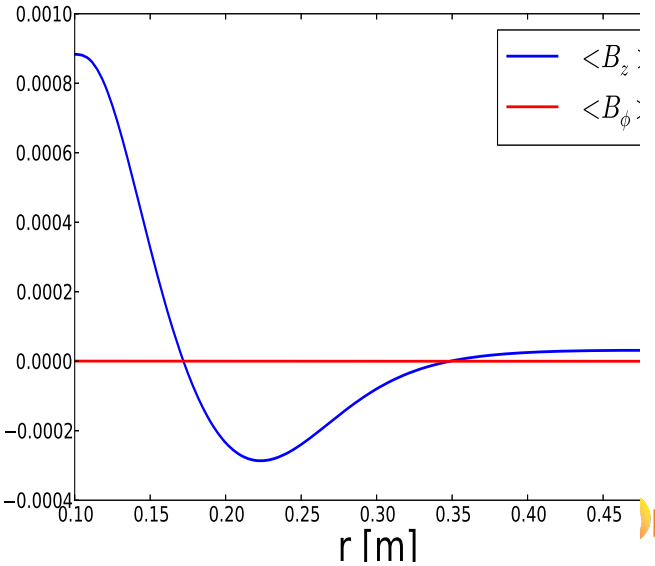

Initial uniform seed B fields toroidally stretched, but due to symmetry, $< B_\phi >$ =0. $\overline{\mathcal{E}} \cdot B = 0$

B_z is amplified due to $\overline{\mathcal{E}}_\phi$.

PPPL PRINCETON UNIVERSITY

Mean toroidal field is generated in the presence of helical perturbation (3-D simulations)

- Field line visualizations during non-linear MRI simulations in a 3D cylinder when m = 1 mode perturbation is dominant.
- Toroidal top view in 3D shows the twisting of the field lines.

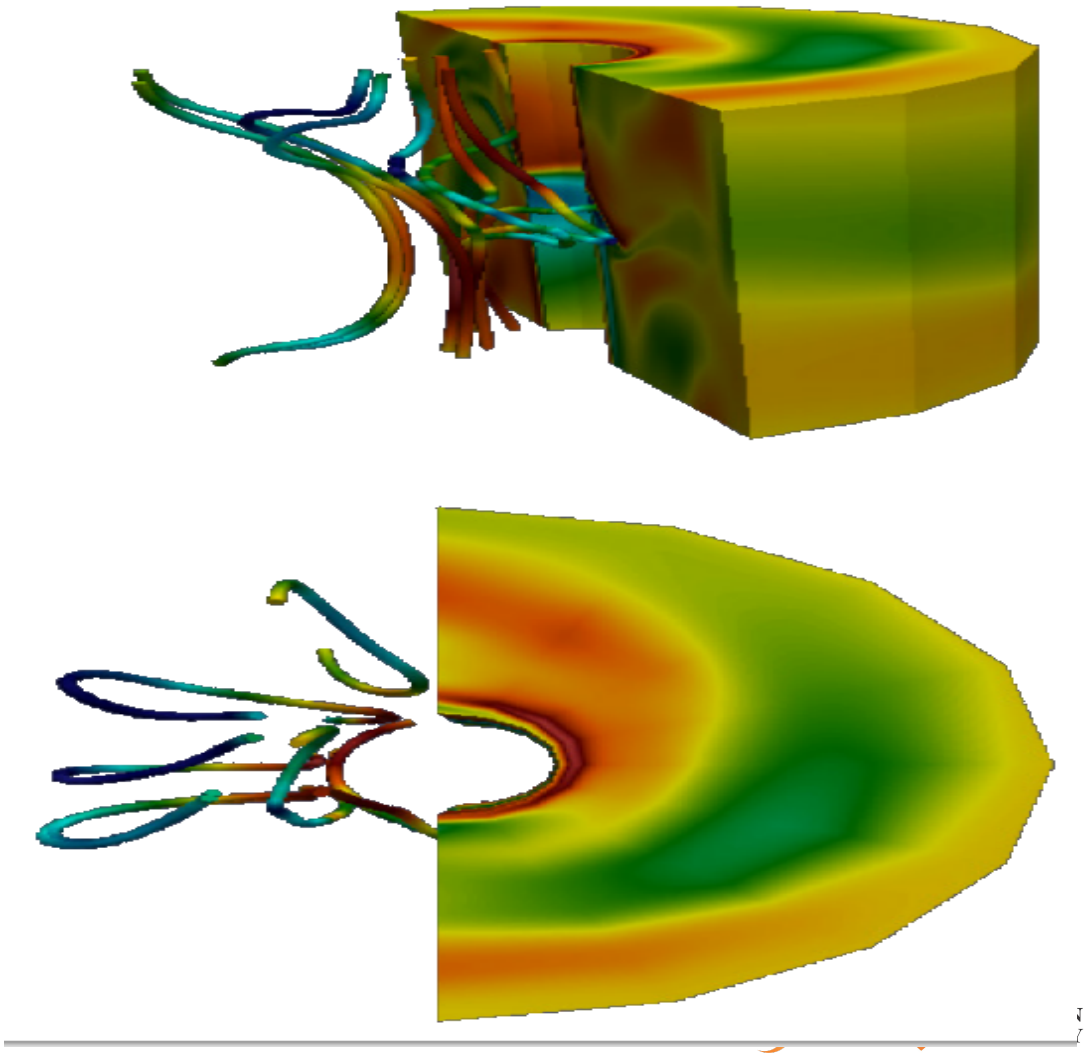

Energy in both large-scale and small-scale is generated (3-D simulations)

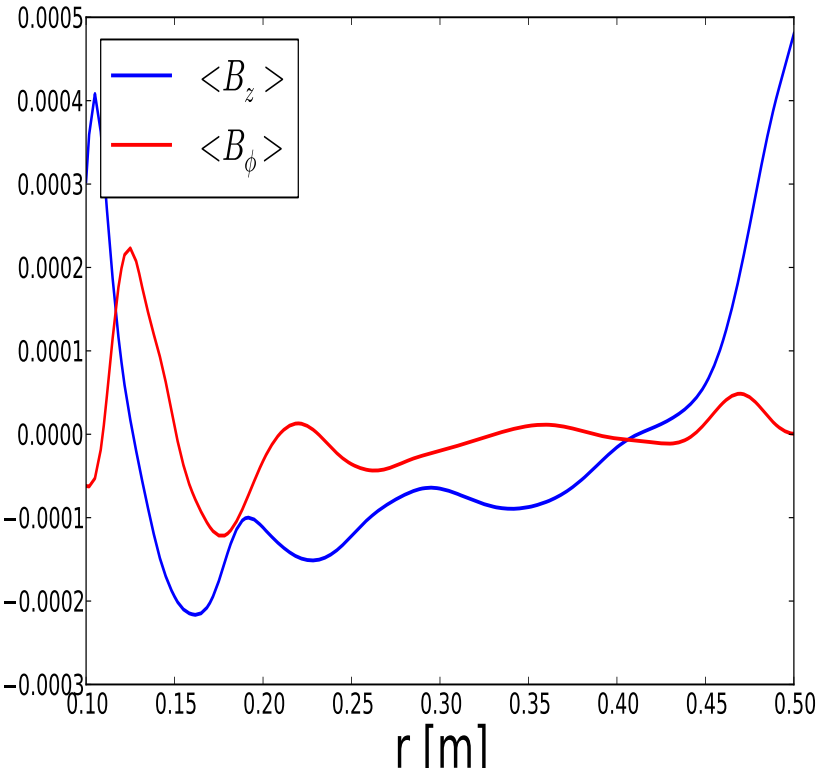

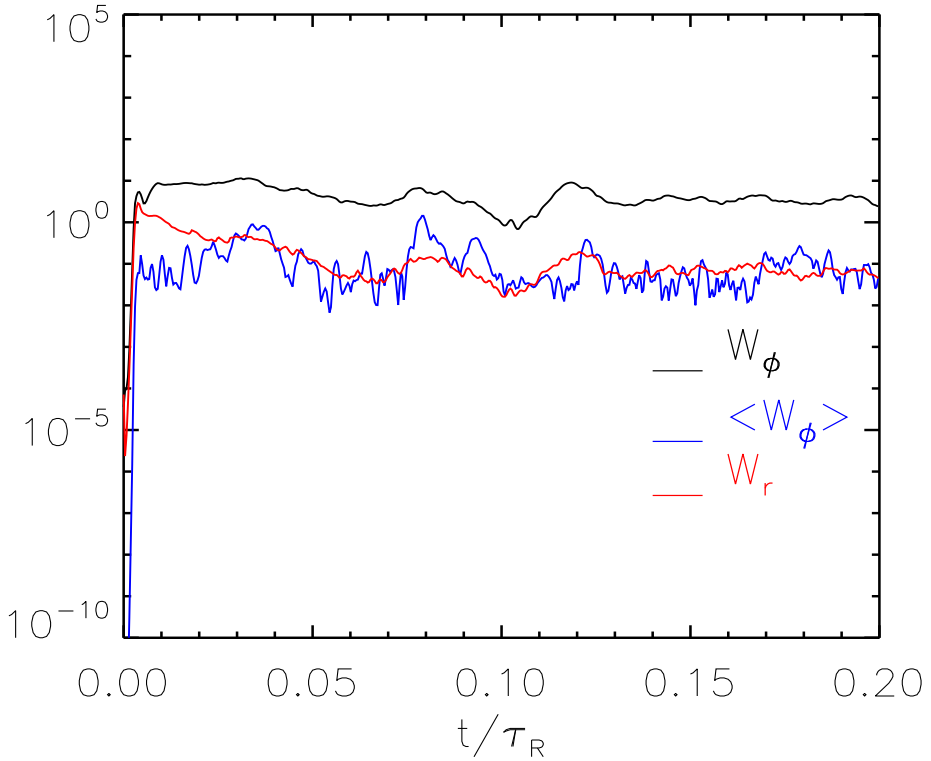

Total magnetic energies, $W_\phi = 1/2 \int B_\phi^2 dr^3$ and large-scale toroidal magnetic energy, $\langle W_\phi \rangle = 1/2 \int \langle B_\phi \rangle^2 dr^3$

PPPL PRINCETON UNIVERSITY

Vertically and toroidally averaged components in our model.

$$\Downarrow = \langle \widetilde{\mathbf{V}} \times \widetilde{\mathbf{B}} \rangle_z$$

$$\frac{\partial \overline{\mathbf{B}_\phi}}{\partial t} = -\frac{\partial \overline{\mathcal{E}}_z}{\partial r} + \underbrace{(\overline{\mathbf{B}} \cdot \nabla)\overline{\mathbf{V}}|_\phi} - (\overline{\mathbf{V}} \cdot \nabla)\overline{\mathbf{B}}|_\phi,$$

$$\Uparrow$$

Traditional Ω effect = $\overline{B_r} V'_\phi$

$$\frac{\partial \overline{\mathbf{B}_r}}{\partial t} = -\frac{\partial \overline{\mathcal{E}}_\phi}{\partial z} + \frac{\partial \overline{\mathcal{E}}_z}{\partial \phi} + (\overline{\mathbf{B}} \cdot \nabla)\overline{\mathbf{V}}|_r - (\overline{\mathbf{V}} \cdot \nabla)\overline{\mathbf{B}}|_r$$

$$\frac{\partial \overline{\mathbf{B}_z}}{\partial t} = \frac{\partial \overline{\mathcal{E}}_\phi}{\partial r} + (\overline{\mathbf{B}} \cdot \nabla)\overline{\mathbf{V}}|_z - (\overline{\mathbf{V}} \cdot \nabla)\overline{\mathbf{B}}|_z$$

PPPL PRINCETON UNIVERSITY

Mean B_ϕ is generated through the vertical EMF, not the traditional Ω effect.

$$\Downarrow = \langle \widetilde{\mathbf{V}} \times \widetilde{\mathbf{B}} \rangle_z$$

$$\frac{\partial \overline{\mathbf{B}}_\phi}{\partial t} = -\frac{\partial \overline{\mathcal{E}}_z}{\partial r} + \cancel{(\overline{\mathbf{B}} \cdot \nabla)\overline{\mathbf{V}}|_\phi} - \cancel{(\overline{\mathbf{V}} \cdot \nabla)\overline{\mathbf{B}}|_\phi},$$

$$\Uparrow$$

Traditional Ω effect = $\bar{B}_r V'_\phi$

$$\frac{\partial \overline{\mathbf{B}}_r}{\partial t} = -\cancel{\frac{\partial \overline{\mathcal{E}}_\phi}{\partial z}} + \cancel{\frac{\partial \overline{\mathcal{E}}_z}{\partial \phi}} + \cancel{(\overline{\mathbf{B}} \cdot \nabla)\overline{\mathbf{V}}|_r} - \cancel{(\overline{\mathbf{V}} \cdot \nabla)\overline{\mathbf{B}}|_r}$$

$$\frac{\partial \overline{\mathbf{B}}_z}{\partial t} = \frac{\partial \overline{\mathcal{E}}_\phi}{\partial r} + \cancel{(\overline{\mathbf{B}} \cdot \nabla)\overline{\mathbf{V}}|_z} - \cancel{(\overline{\mathbf{V}} \cdot \nabla)\overline{\mathbf{B}}|_z}$$

PPPL PRINCETON UNIVERSITY

DNS shows that mean toroidal field is correlated with, and directly generated by the vertical EMF.

From Direct numerical simulations

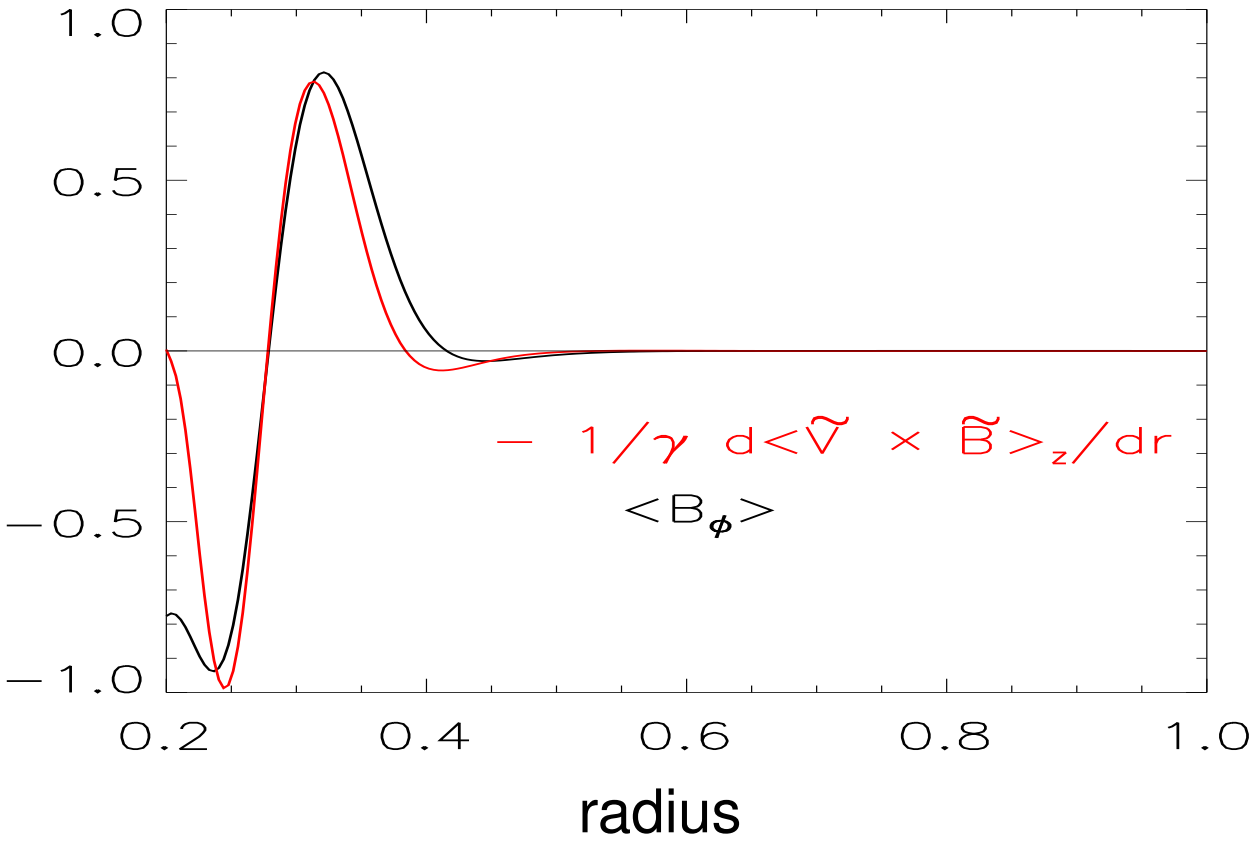

- $\frac{\partial \overline{\mathbf{B}_\phi}}{\partial t} = -\frac{\partial \overline{\mathcal{E}}_z}{\partial r}$ see more analytical calculations in Ebrahimi & Blackman 2016

PPPL PRINCETON UNIVERSITY

The dynamo effect is closely related to magnetic helicity transport

- What is the form of fluctuation-induced emf force?
- Can fluctuations inject magnetic helicity and generate flux?
- Do local magnetic helicity fluxes sustain large scale dynamo?

  [F. Ebrahimi and A. Bhattacharjee PRL 2014]

PPPL PRINCETON UNIVERSITY

The alpha effect can be rigorously written in the form of a total divergence of the helicity flux from fluctuations

Local magnetic helicity variation is

$$\frac{\partial(\mathbf{A}\cdot\mathbf{B})}{\partial t}+\nabla\cdot\Gamma_k=-2\mathbf{E}\cdot\mathbf{B}.$$

Total helicity flux : $\Gamma_k=-2\mathbf{A}\times\mathbf{E}-\mathbf{A}\times\frac{\partial\mathbf{A}}{\partial t}$

- It can be shown that fluctuation induced dynamo effect is expressed in a divergence form and dissipative terms.

$$\varepsilon_{emf}\cdot\overline{\mathbf{B}}=-\eta<\widetilde{\mathbf{J}}\cdot\widetilde{\mathbf{B}}>-\frac{1}{2}\frac{\partial}{\partial t}<\widetilde{\mathbf{A}}\cdot\widetilde{\mathbf{B}}>+H\alpha$$

Where;

$$H\alpha=-\frac{1}{2}\nabla\cdot<\Gamma_k>=\nabla\cdot[<\widetilde{\mathbf{A}}\times\widetilde{\mathbf{E}}>+\frac{1}{2}<\widetilde{\mathbf{A}}\times\frac{\partial}{\partial t}\widetilde{\mathbf{A}}>]$$

PPPL PRINCETON UNIVERSITY

Nonlinear simulations show that the alpha effect can be written in terms of a total divergence for an MRI mode.

Magnetic energies

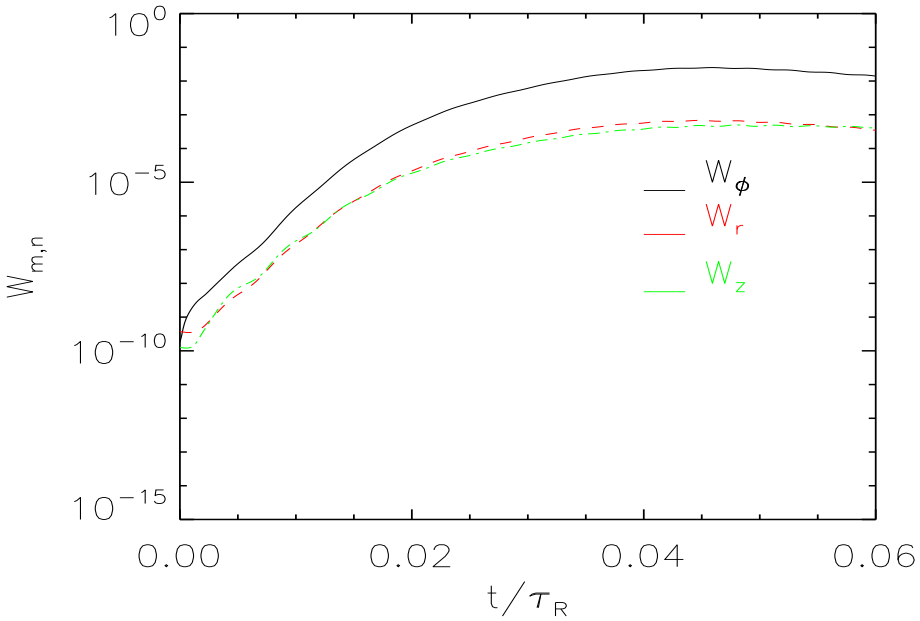

m=1 MRI dynamo

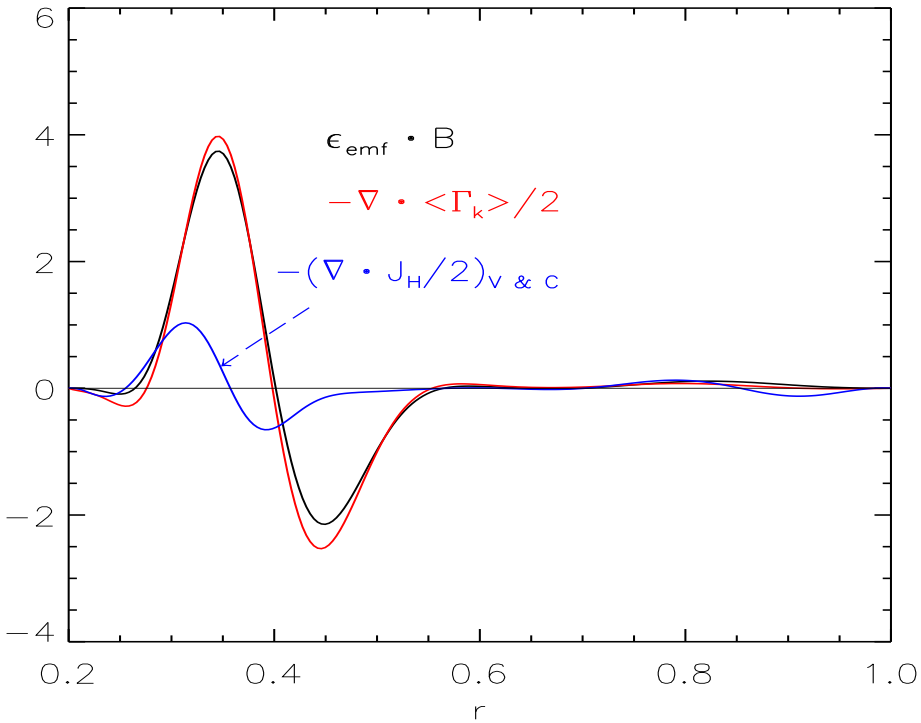

- Nonlinear m=1 MRI mode simulations show $< \widetilde{\mathbf{V}} \times \widetilde{\mathbf{B}} > \cdot \overline{\mathbf{B}} \approx -\nabla \cdot < \Gamma_k > /2$.

PPPL PRINCETON UNIVERSITY

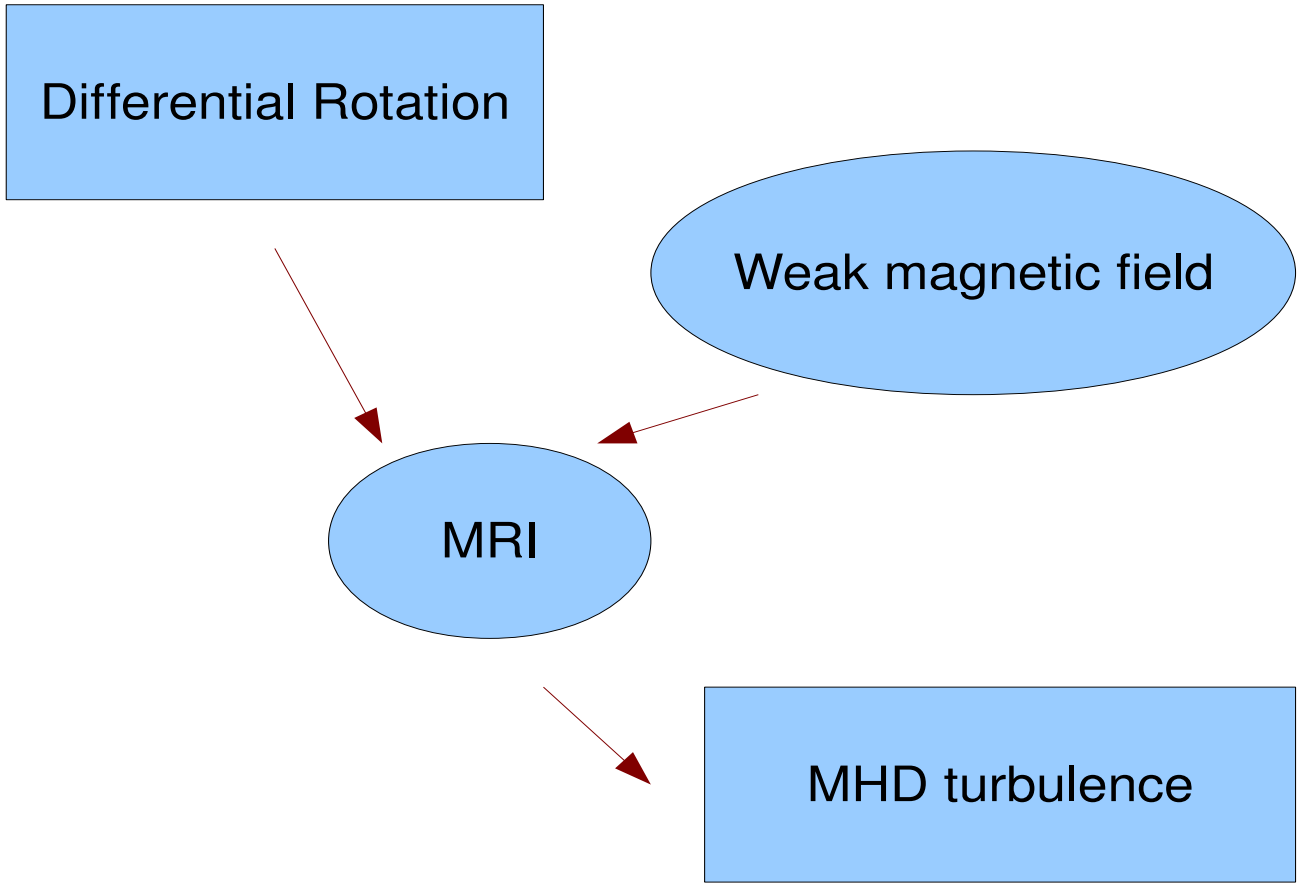
Differential Rotation
Weak magnetic field
MRI
MHD turbulence

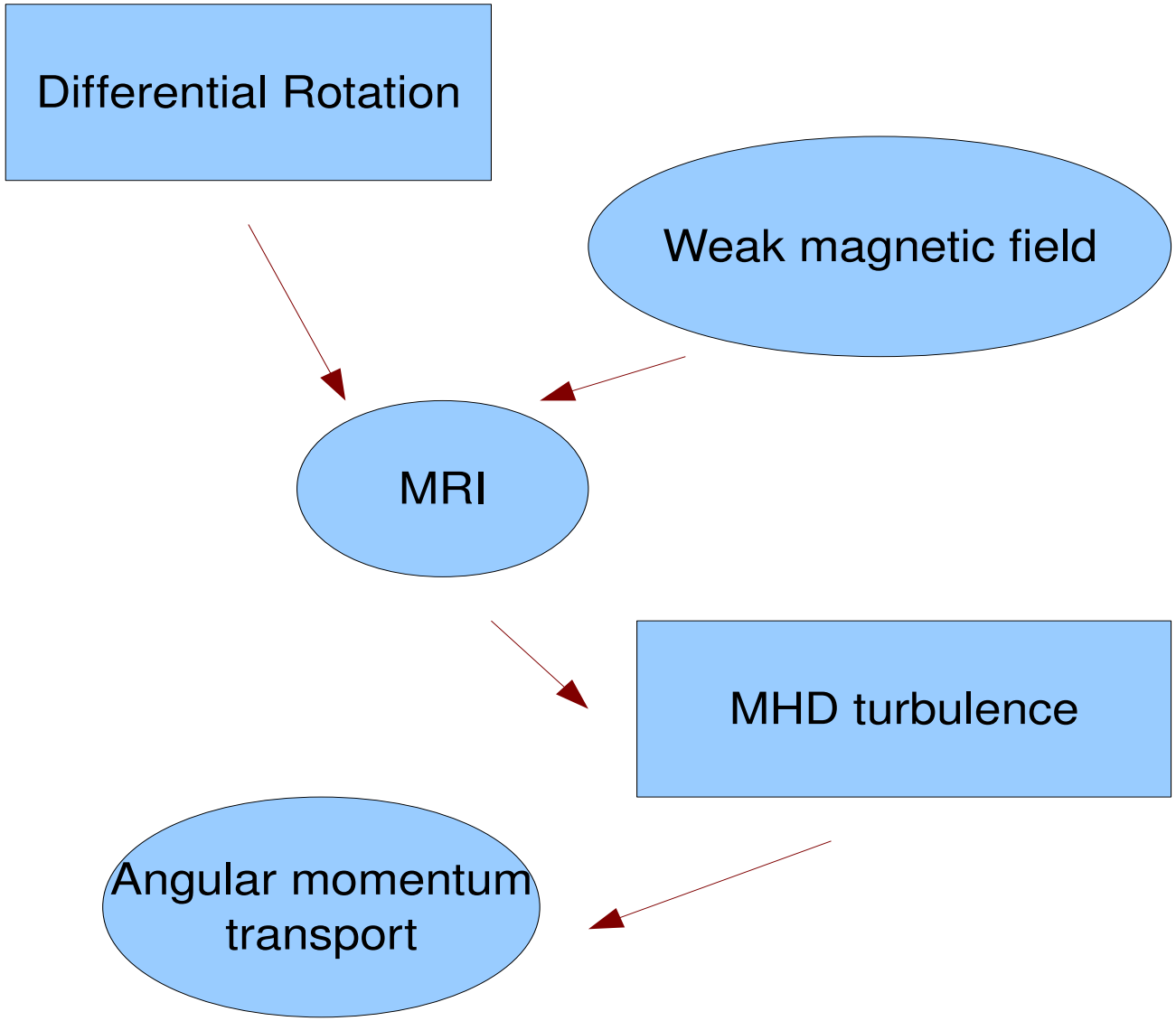
Differential Rotation
Weak magnetic field
MRI
MHD turbulence
Angular momentum transport

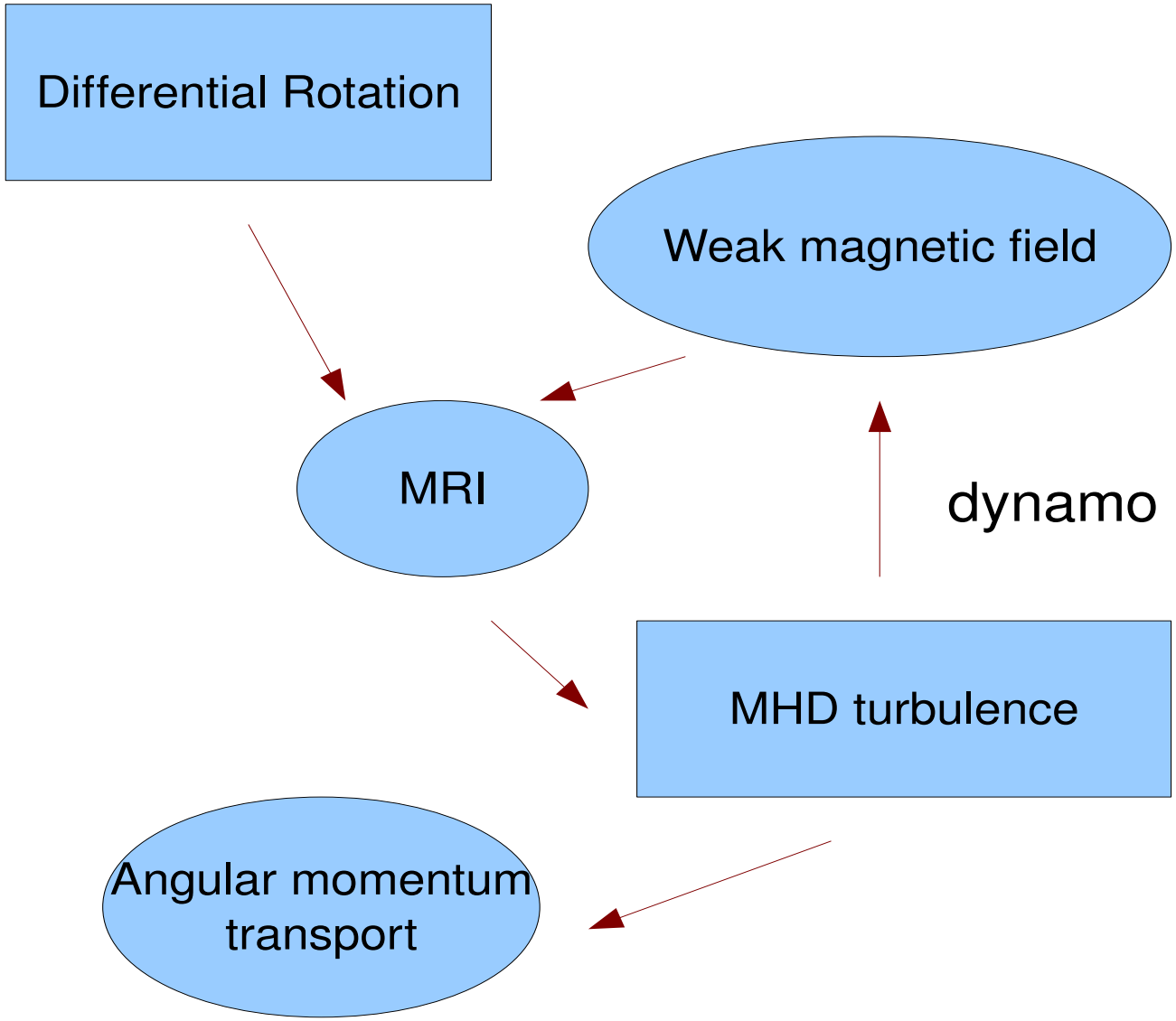
Differential Rotation
Weak magnetic field
MRI
dynamo
MHD turbulence
Angular momentum transport

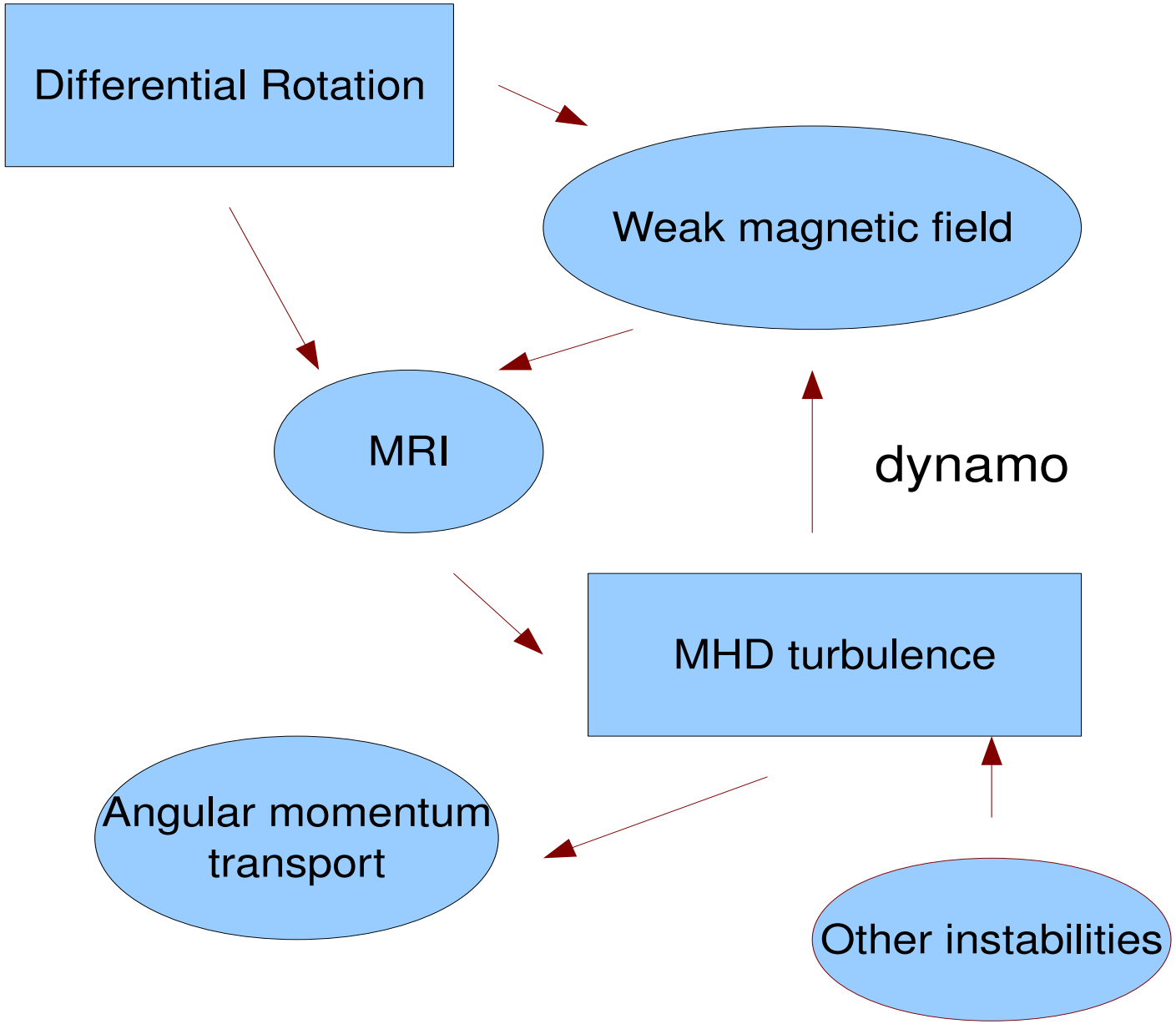

PPPL PRINCETON UNIVERSITY

How could nature get rid of all the magnetic helicities?

Nature tries to get rid of magnetic helicity through magnetic reconnection

Would magnetic field be annihilated while being generated?

Magnetic reconnection:

- energizes many processes in nature
- is a major interplay for fundamental physical phenomena such as particle acceleration and heating, magnetic-field generation, and momentum transport

PPPL PRINCETON UNIVERSITY

Magnetic reconnection is the rearrangement of magnetic field topology of plasmas – forced (driven) reconnection

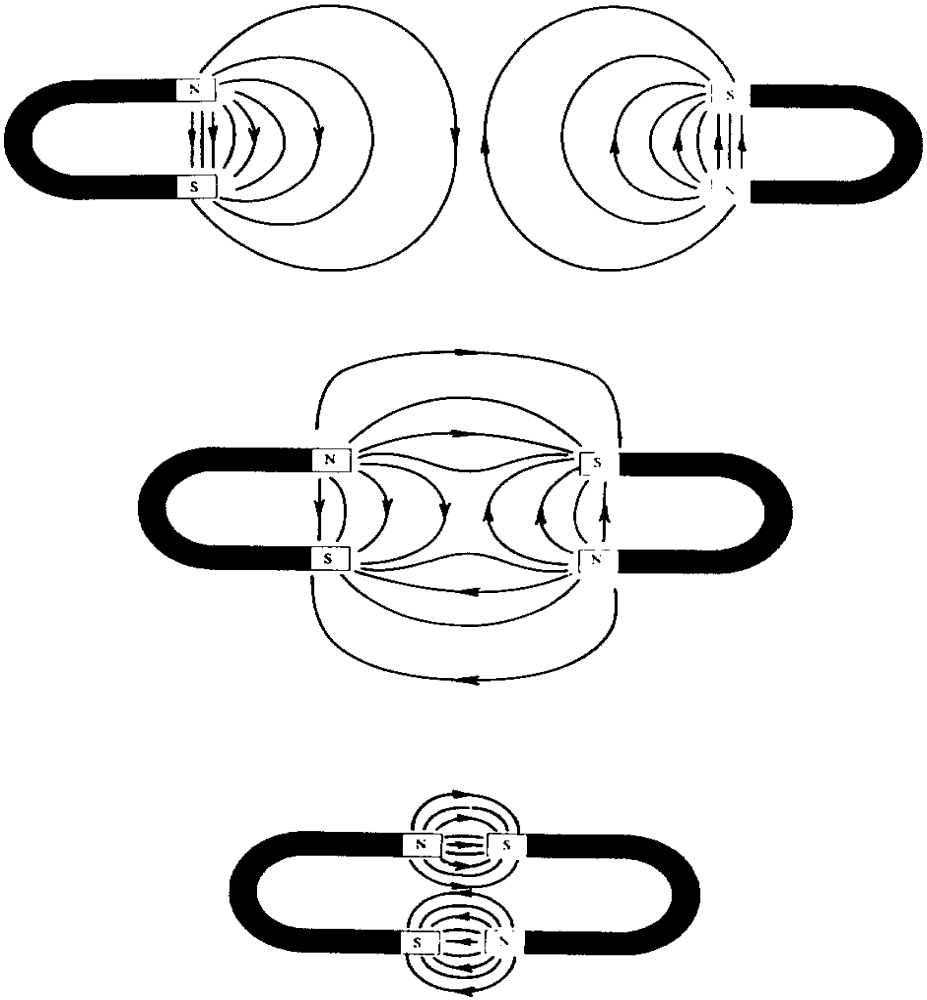

This process occurs in the solar atmosphere, the solar wind, the Earth's magnetosphere, astrophysical disks, turbulence, and laboratory plasmas.

PPPL PRINCETON UNIVERSITY

Magnetic reconnection is the rearrangement of magnetic field topology of plasmas.

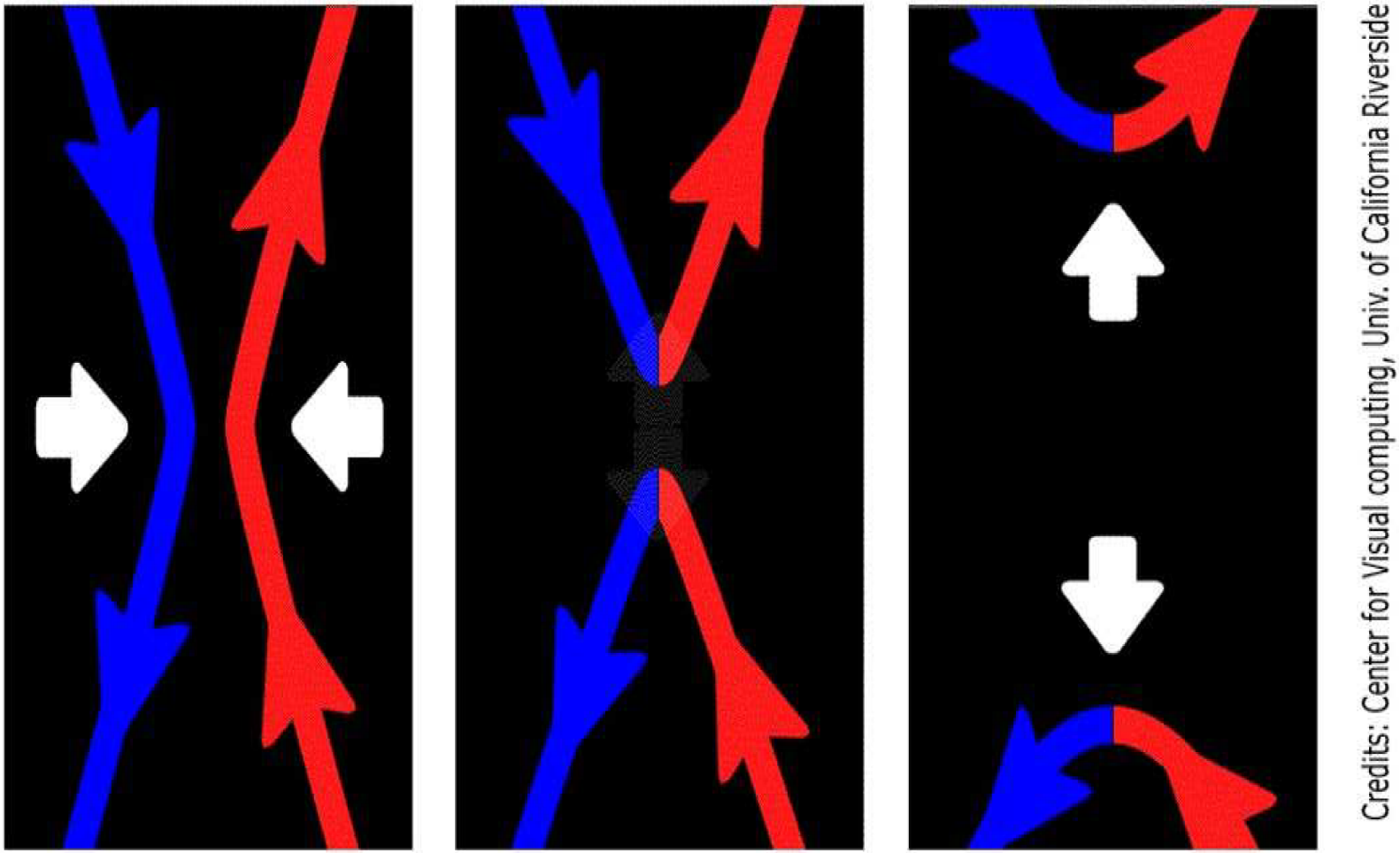

Credits: Center for Visual computing, Univ. of California Riverside

PPPL PRINCETON UNIVERSITY

Current-driven magnetic reconnection - Tearing instability
Spontaneous reconnection

Furth, Killeen, and Rosenbluth (1963)

THE PHYSICS OF FLUIDS

VOLUME 6, NUMBER 4 APRIL 1963

Finite-Resistivity Instabilities of a Sheet Pinch

HAROLD P. FURTH AND JOHN KILLEEN
Lawrence Radiation Laboratory, Livermore, California
AND
MARSHALL N. ROSENBLUTH
University of California, San Diego, La Jolla, California, and *John Jay Hopkins Laboratory for Pure and Applied Science, General Atomic Division of General Dynamics Corporation, San Diego, California*
(Received 17 September 1962)

The stability of a plane current layer is analyzed in the hydromagnetic approximation, allowing for finite isotropic resistivity. The effect of a small layer curvature is simulated by a gravitational field. In an incompressible fluid, there can be three basic types of "resistive" instability: a long-wave "tearing" mode, corresponding to breakup of the layer along current-flow lines; a short-wave "rippling" mode, due to the flow of current across the resistivity gradients of the layer; and a low-g gravitational interchange mode that grows in spite of finite magnetic shear. The time scale is set by the resistive diffusion time τ_R and the hydromagnetic transit time τ_H of the layer. For large $S = \tau_R/\tau_H$, the growth rate of the "tearing" and "rippling" modes is of order $\tau_R^{-3/5}\tau_H^{-2/5}$, and that of the gravitational mode is of order $\tau_R^{-1/3}\tau_H^{-2/3}$. As $S \to \infty$, the gravitational effect dominates and may be used to stabilize the two nongravitational modes. If the zero-order configuration is in equilibrium, there are no overstable modes in the incompressible case. Allowance for plasma compressibility somewhat modifies the "rippling" and gravitational modes, and may permit overstable modes to appear. The existence of overstable modes depends also on increasingly large *zero-order* resistivity gradients as $S \to \infty$. The three unstable modes merely require increasingly large gradients of the *first-order* fluid velocity; but even so, the hydromagnetic approximation breaks down as $S \to \infty$. Allowance for isotropic viscosity increases the effective mass density of the fluid, and the growth rates of the "tearing" and "rippling" modes then scale as $\tau_R^{-2/3}\tau_H^{-1/3}$. In plasmas, allowance for thermal conductivity suppresses the "rippling" mode at moderately high values of S. The "tearing" mode can be stabilized by conducting walls. The transition from the low-g "resistive" gravitational mode to the familiar high-g infinite conductivity mode is examined. The extension of the stability analysis to cylindrical geometry is discussed. The relevance of the theory to the results of various plasma experiments is pointed out. A nonhydromagnetic treatment will be needed to achieve rigorous correspondence to the experimental conditions.

I. INTRODUCTION

A PRINCIPAL result of pinch[1,2] and stellarator[3] research has been the observed instability of configurations that the hydromagnetic theory[4,5] would predict to be stable in the limit of high electrical conductivity. In order to establish the cause of this observed instability, the extension of the hydromagnetic analysis to the case of finite conductivity becomes of considerable interest.

A number of particular "resistive" instability modes have been discussed in previous publications. Dungey[6] has shown that, at an x-type neutral point of a magnetic field structure in plasma of finite

[1] S. A. Colgate and H. P. Furth, Phys. Fluids **3**, 982 (1960).
[2] K. Aitken, R. Bickerton, R. Hardcastle, J. Jukes, P. Reynolds, and S. Spalding, IAEA Conference on Plasma

PRINCETON UNIVERSITY

Spontaneous magnetic reconnection as the result of tearing fluctuations

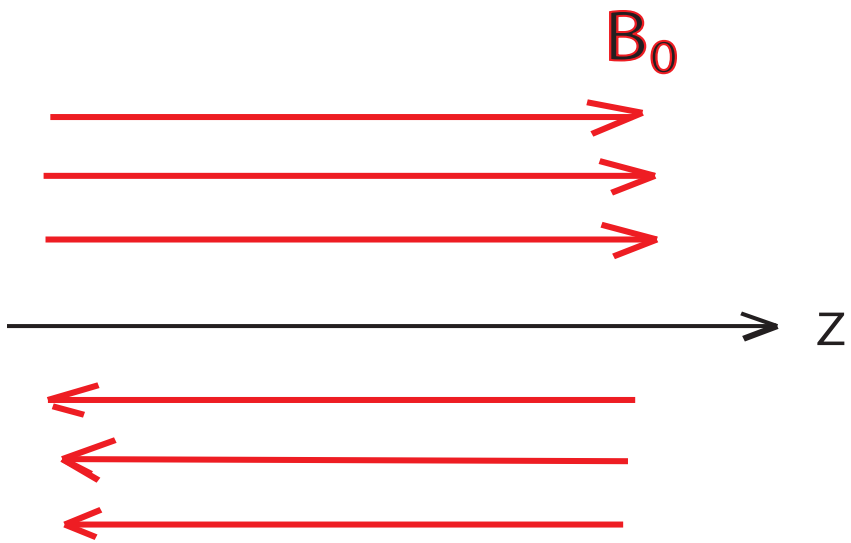

with small perturbation

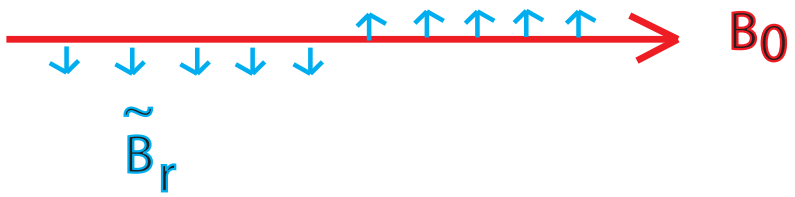

PPPL PRINCETON UNIVERSITY

Magnetic reconnection

if $\eta = 0$

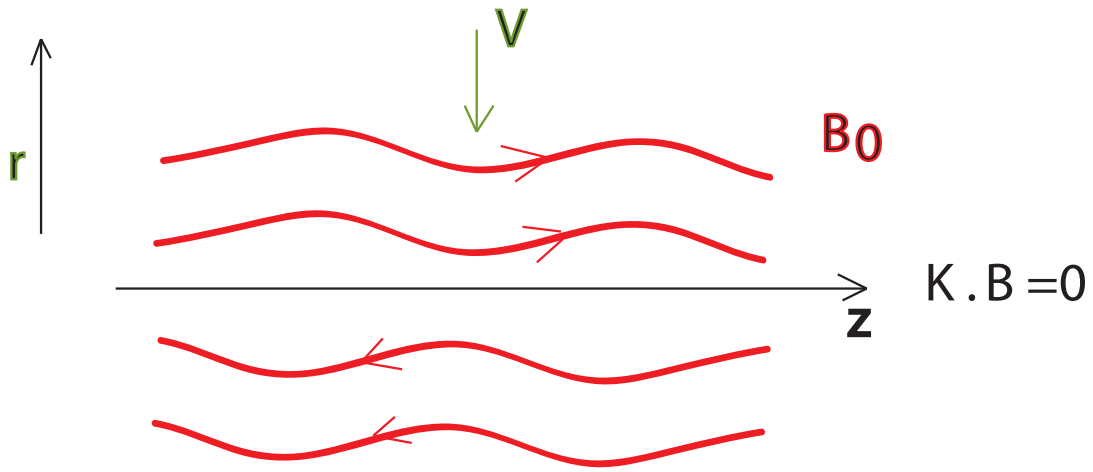

$$\frac{d\mathbf{B}}{dt} = \nabla \times (\mathbf{V} \times \mathbf{B})$$

$$\widetilde{V}_r = \gamma \widetilde{B}_r / (k \cdot B) ===> \boxed{\widetilde{B}_r = 0}$$

Magnetic reconnection occurs at finite resistivity

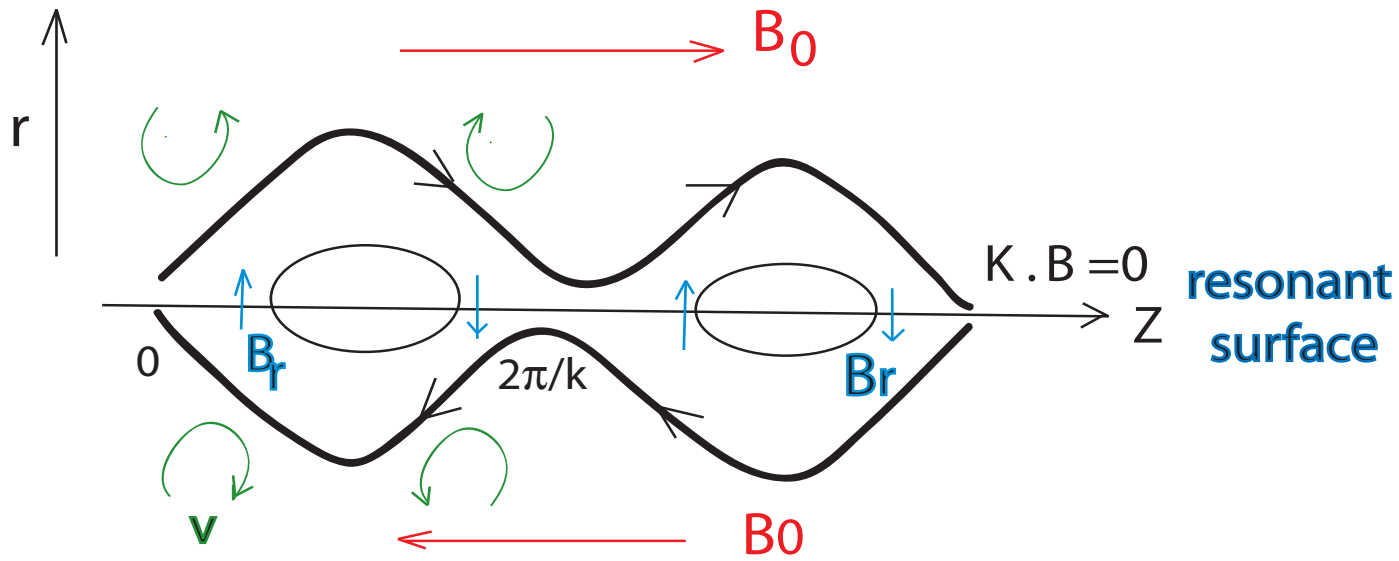

magnetic diffusion equation:

$$\frac{d\mathbf{B}}{dt} = \nabla \times (\mathbf{V} \times \mathbf{B}) - \frac{\eta}{\mu_0} \nabla^2 \mathbf{B}$$

- $\widetilde{B}_r(\mathbf{r}, t) \sim \widetilde{B}_r(r) \exp(ik_z z - i\omega t)$

Magnetic Reynolds number a measure of how closely the magnetic field is coupled to the fluid

Dimensionless equation

$$\frac{d\mathbf{B}}{dt} = S\nabla \times (\mathbf{V} \times \mathbf{B}) - \eta \nabla^2 \mathbf{B}$$

measure of plasma resistivity, Lundquist number $S = \tau_R/\tau_A$

$\tau_R = \mu_0 a^2/\eta \quad \tau_A = a/(B^2/(\mu_0\rho)^{1/2})$

Growth rate is a hybrid between resistive and Alfven times:

$\tau_{growth} \sim \tau_R^{-3/5}\tau_A^{-2/5}$, $\gamma\tau_A \propto S^{-3/5}$

In general magnetic Reynolds number $Rm \equiv LV/\eta$

PPPL PRINCETON UNIVERSITY

Many fundamentals of reconnection physics can be explored during helicity injection

Solar flares field lines modeling

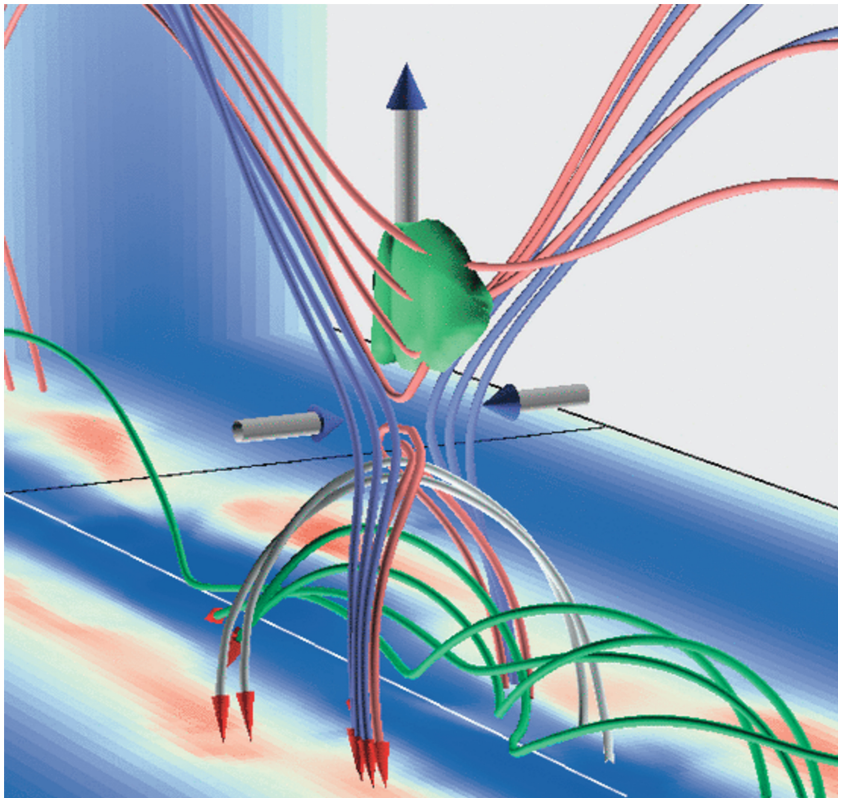

$$\frac{\partial K}{\partial t} = -2 \int (\mathbf{A}.\mathbf{V})\mathbf{B} \cdot d\mathbf{s}$$

Kusano 2004

Warnecke & Brandenburg 2010

Helicity injection in a lab

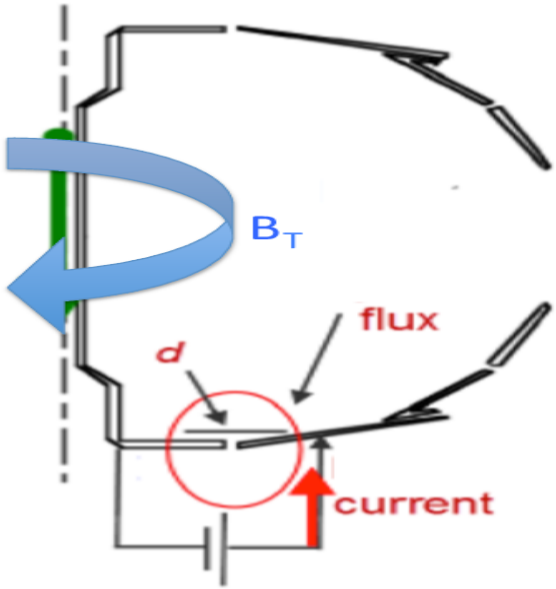

$$\frac{\partial K}{\partial t} = -2 \int \Phi \mathbf{B} \cdot d\mathbf{s}$$

Helicity is injected through a surface term.

PPPL PRINCETON UNIVERSITY

Transient Coaxial Helicity Injection (CHI), the primary candidate for solenoid- free current start-up in spherical tokamaks

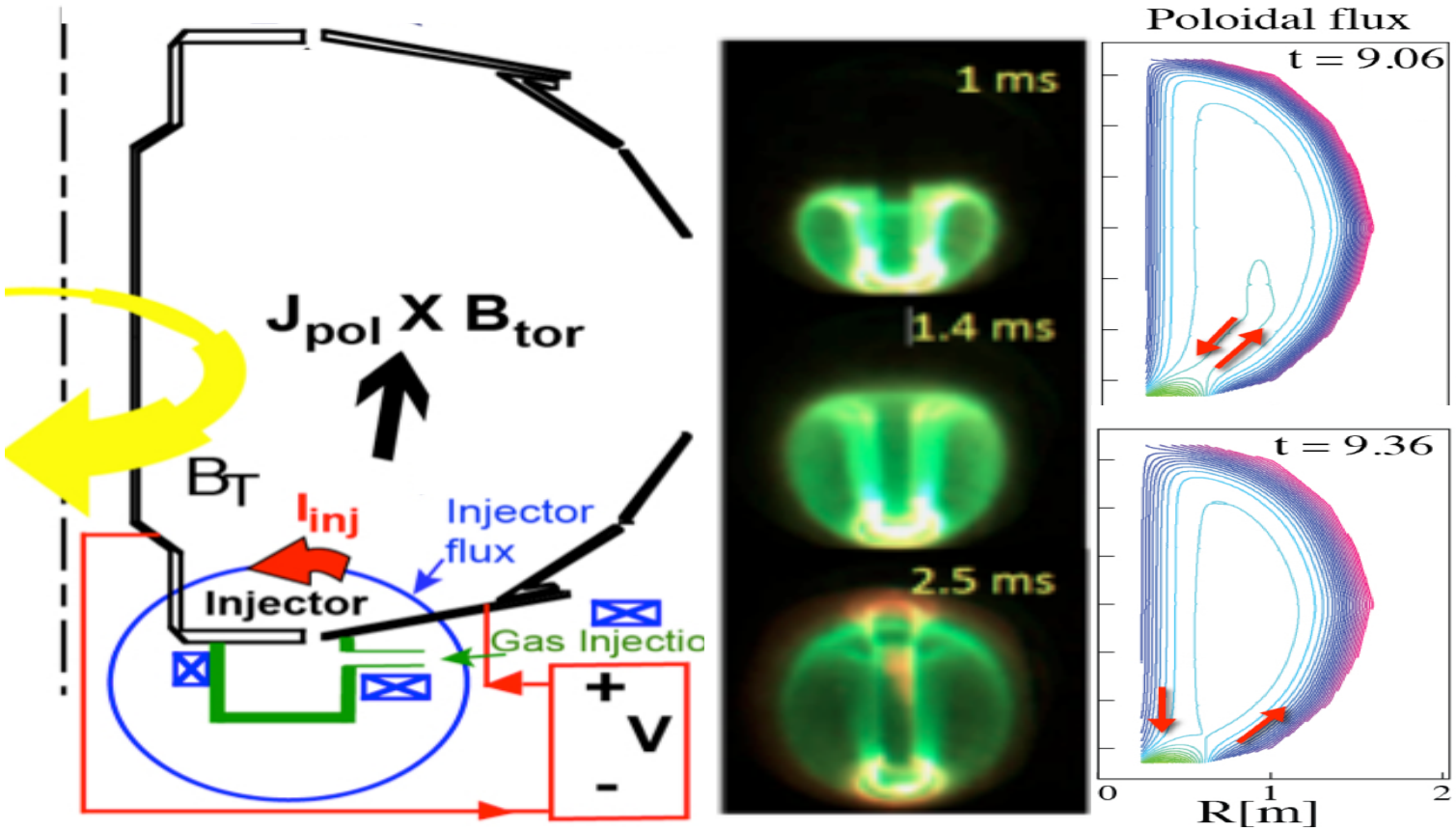

Helicity injection simulations are performed using the extended-MHD NIMROD code

- Solves the linear and nonlinear MHD equations

$$\begin{aligned}
\frac{\partial \mathbf{B}}{\partial t} &= -\nabla \times \mathbf{E} + \kappa_{divb} \nabla \nabla . \mathbf{B} \\
\mathbf{E} &= -\mathbf{V} \times \mathbf{B} + \eta \mathbf{J} + \frac{1}{ne} \mathbf{J} \times \mathbf{B} \\
\mathbf{J} &= \nabla \times \mathbf{B} \\
\frac{\partial n}{\partial t} + \nabla . (n\mathbf{V}) &= \nabla . D \nabla n \\
\rho (\frac{\partial \mathbf{V}}{\partial t} + \mathbf{V} . \nabla \mathbf{V}) &= \mathbf{J} \times \mathbf{B} - \nabla P - \nabla . \Pi \\
\frac{n}{(\Gamma - 1)} (\frac{\partial T_\alpha}{\partial t} + \mathbf{V} . \nabla T_\alpha) &= -p_\alpha \nabla . \mathbf{V} - \nabla . \mathbf{q}_\alpha + Q
\end{aligned}$$

- $\mathbf{q} = -n[(\kappa_{||} - \kappa_\perp)\hat{b}\hat{b} + \kappa_\perp \mathbf{I}] \cdot \nabla T$
- Π is the stress tensor (also includes numerical $\rho \nu \nabla V$)
- κ_{divb} and D are magnetic-divergence and density diffusivities for numerical purposes

PPPL PRINCETON UNIVERSITY

Reconnection could occur during both stages of helicity injection

During injection (V_{inj} on)

During decay (V_{inj} =0)

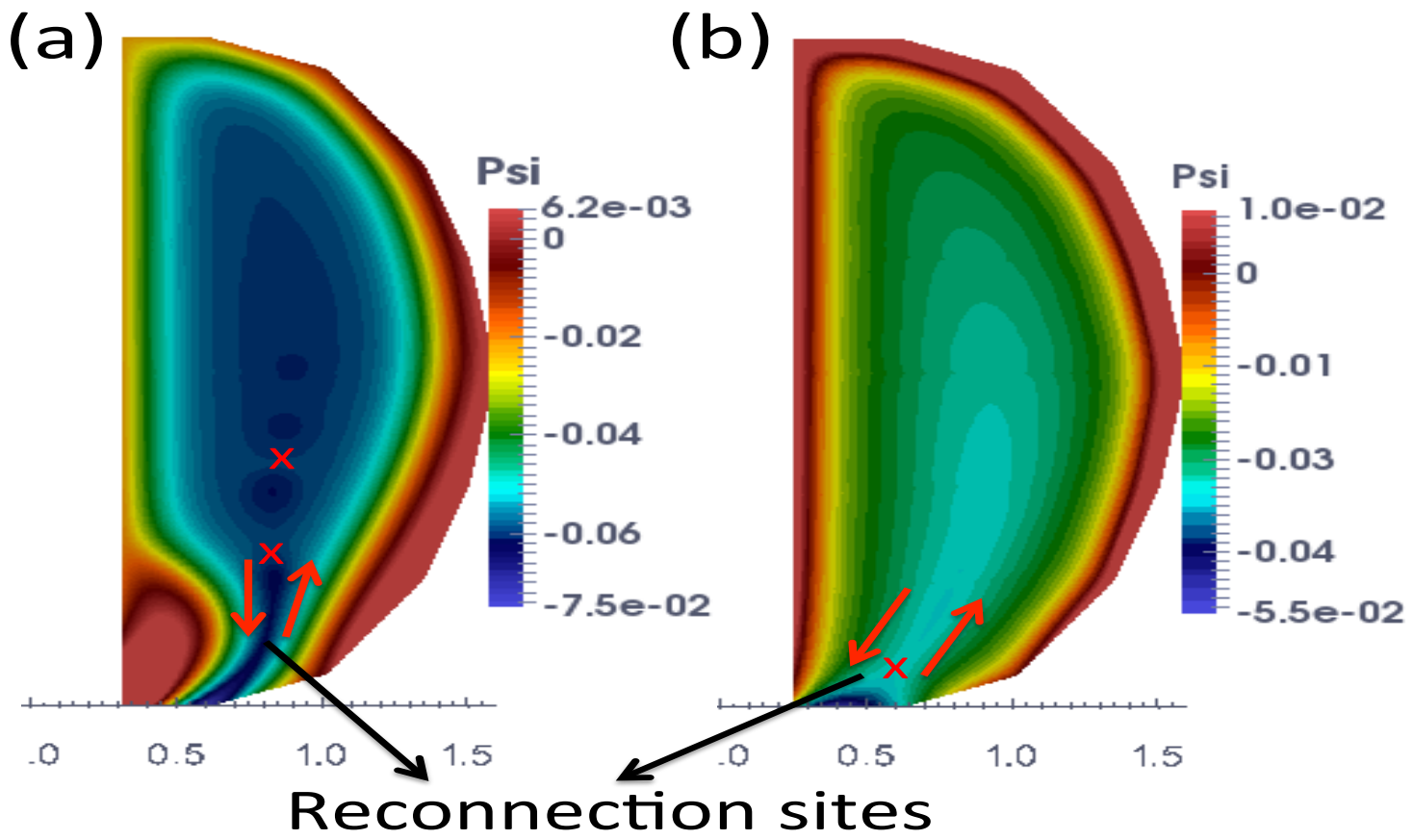

PPPL PRINCETON UNIVERSITY

Two types of current sheets are formed during flux expansion/evolution

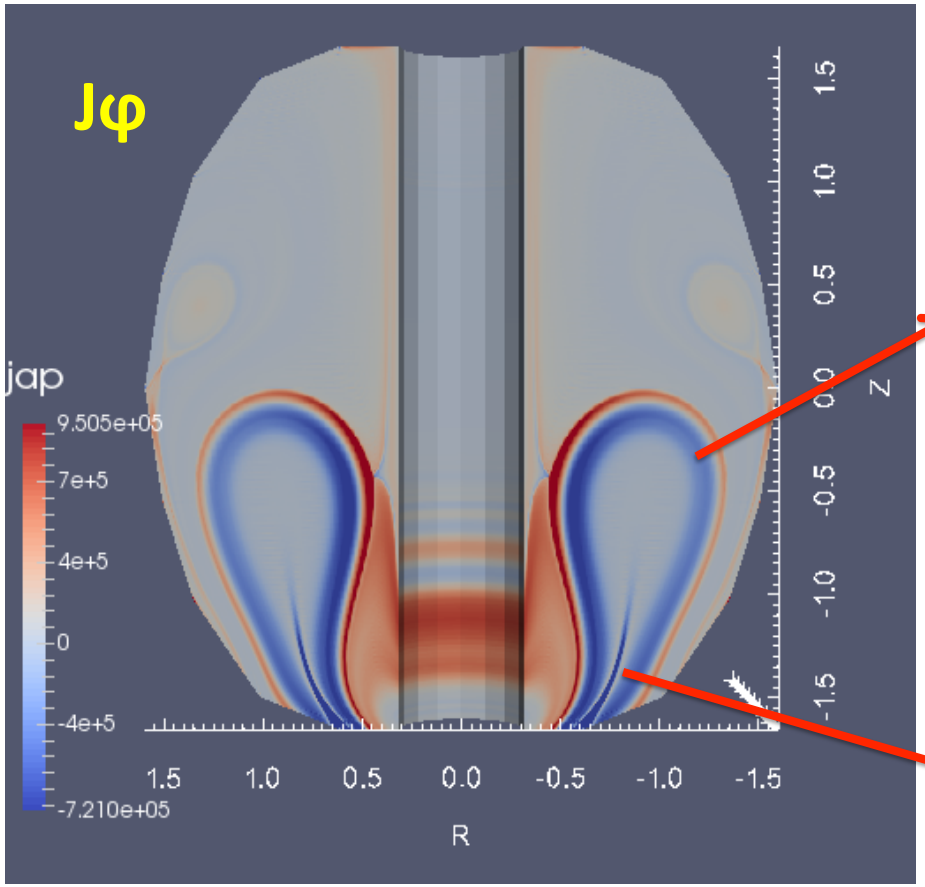

- 1- **Edge current sheet** from the poloidal flux compression near the plasma edge, **leads to 3-D filament structures**
- 2- **Primary reconnecting current sheet** from the oppositely directed field lines in the injector region.

F. Ebrahimi PoP Letters 2016

PPPL PRINCETON UNIVERSITY

Forced reconnection in the injection region

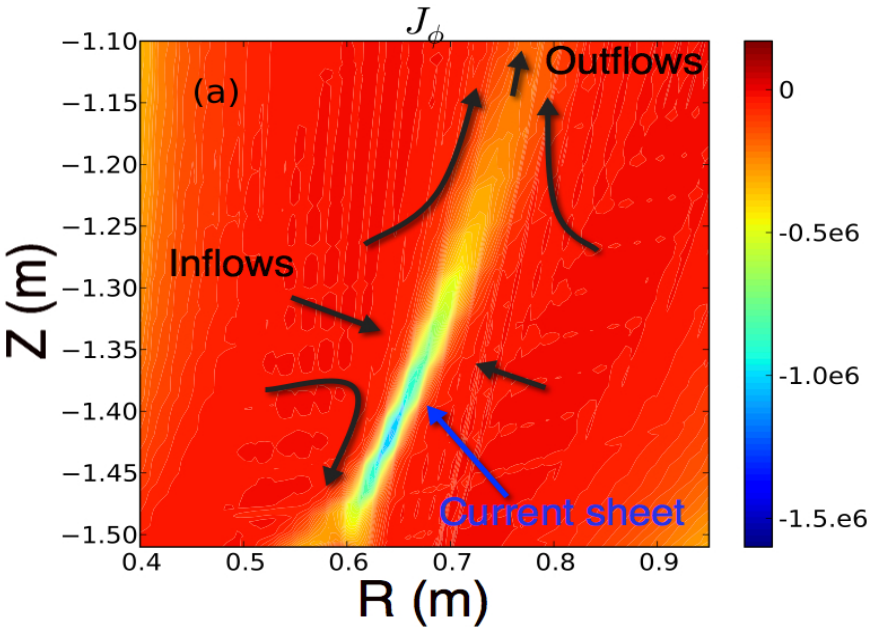

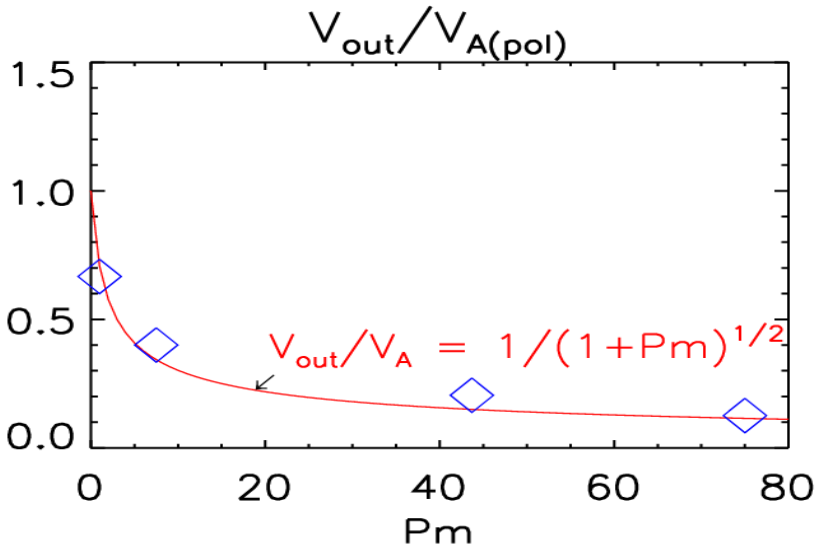

A local 2-D Sweet-Parker type reconnection is triggered in the injection region. Key signatures:

- I - Elongated current sheets, $L > \delta$.
- II - Scaling of the current sheet width $\delta/L \sim (1+P_m)^{1/4} S^{-1/2} \sim V_{in}/V_{out}$
- III -Pinch inflow and Alfvénic outflow

S = LV_A/η (Alfven velocity based on the reconnecting B, L is the current sheet length) F. Ebrahimi, et al. PoP 2013, 2014

PPPL PRINCETON UNIVERSITY

In many fast MHD dynamical processes, plasmoids are essential features

- Elongated current sheet can become tearing unstable at high S. [Biskamp 1986, Shibata & Tanuma 2001]

- The scaling properties of a classical linear tearing changes, ($\gamma \sim S^{1/4}$).
  Numerical development: [Tajima & Shibata 1997,Loureiro et al. 2007; Lapenta 2008; Daughton et al. 2009,; Bhattacharjee et al. 2009] **show fast reconnection**. Static linear theory doesn't apply [L. Comisso et al. PoP 2016]

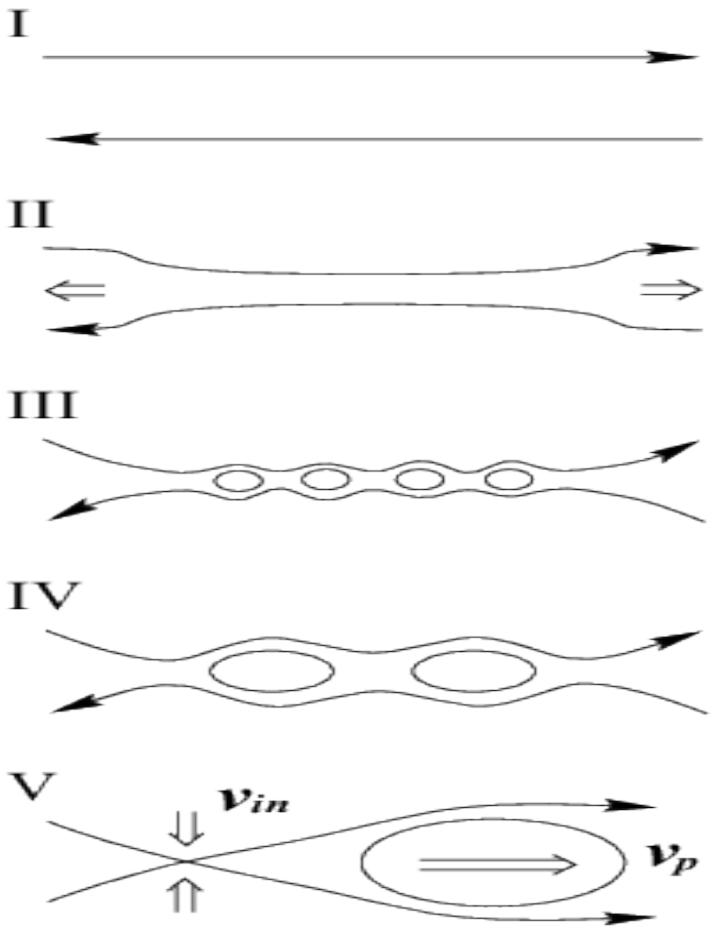

Shibata & Tanuma 2001

PPPL PRINCETON UNIVERSITY

Spontaneous plasmoid reconnection

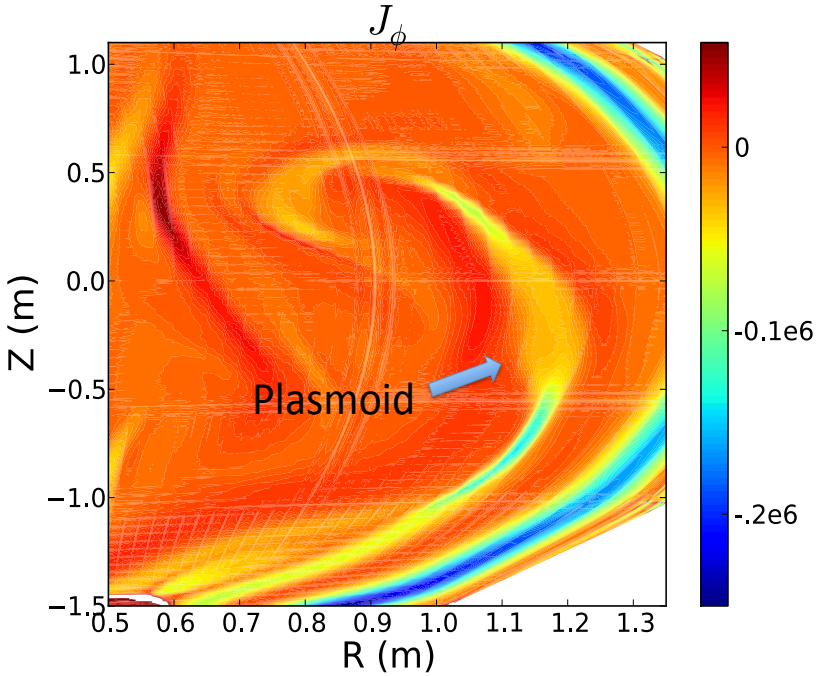

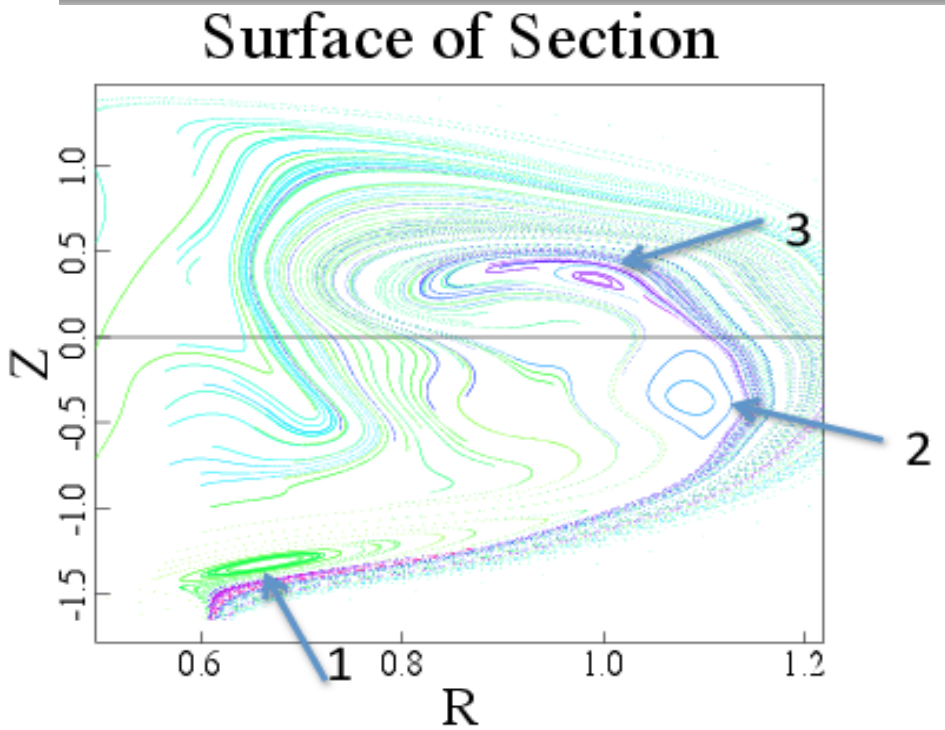

At high S, a transition to a plasmoid instability is demonstrated in the simulations.

Both small sized transient plasmoids and large system-size plasmoids are formed and co-exist. (S=39000)

Plasmoids merge to form closed flux surfaces. Reconnection rate becomes nearly independent of S.

F. Ebrahimi and R.Raman PRL 2015

PPPL PRINCETON UNIVERSITY

Plasmoid instability with continued injection of plasmoids is observed during the injection phase (S $\sim$ 29000)

(Loading poloidalflux.mp4)

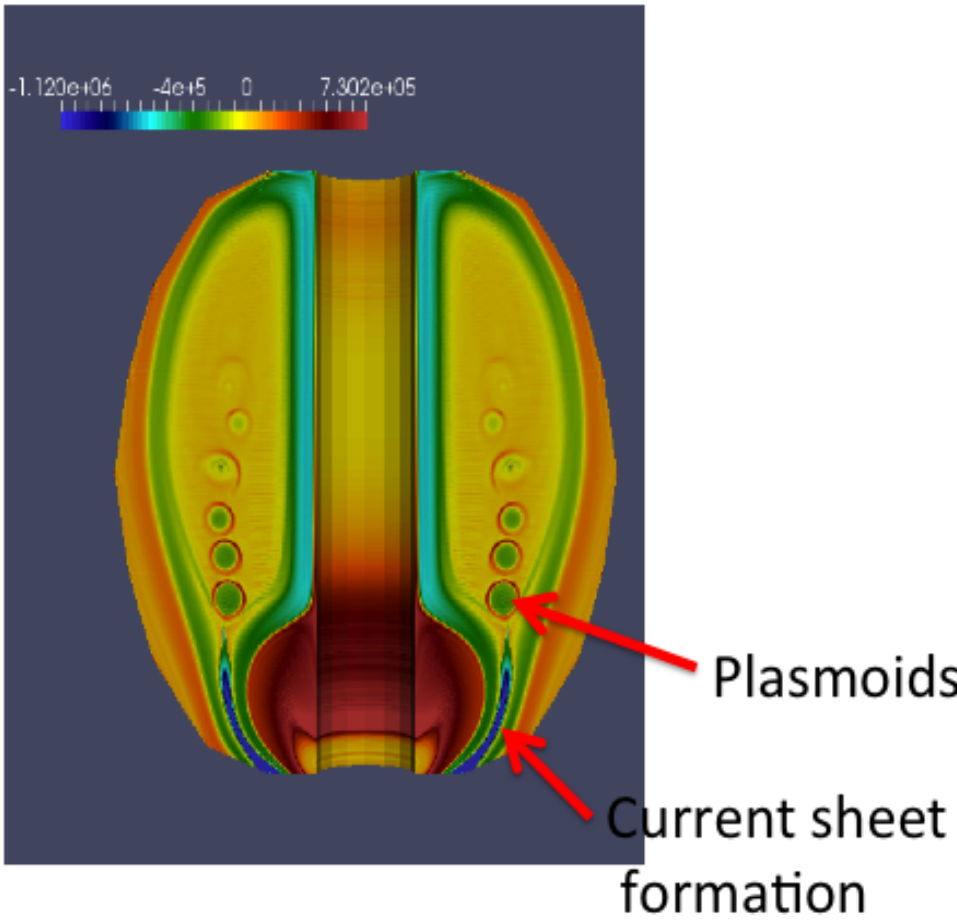

Dynamo-driven plasmoids formation

- 3D effects
  - Could large-scale dynamo from 3-D fluctuations trigger reconnecting plasmoids?
  - Self-consistent trigger mechanism in 3-D?

PPPL PRINCETON UNIVERSITY

Edge current-sheet instabilities are triggered in 3-D, and break the current-sheet

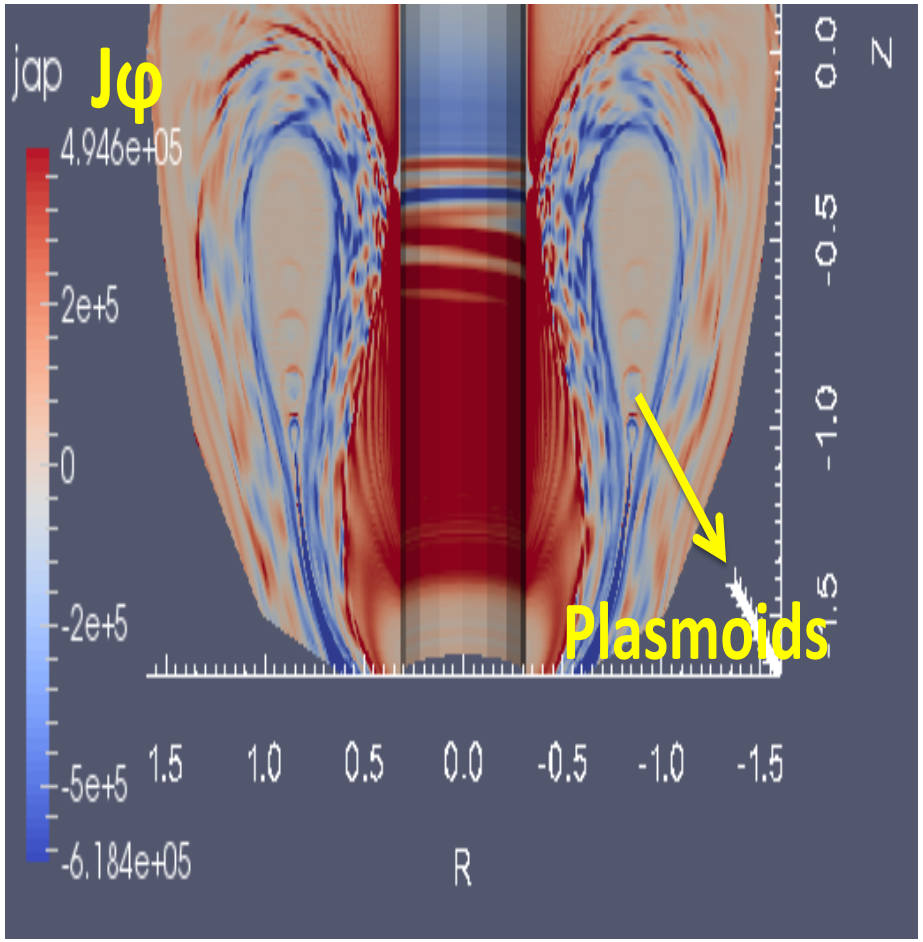

1. I- **Edge-localized modes arising from the asymmetric current-sheet instabilities**
2. II- First observation of nonaxisymmetric edge current
3. III- With 3-D fluctuations, axisymmetric plasmoids are formed, **local S increased to S ∼ 15000.** [Ebrahimi PoP Letters 2016]

PPPL PRINCETON UNIVERSITY

Edge modes grow on the poloidal Alfven time scales

1. These modes grow fast, on the poloidal Alfven time scales, and are **peeling modes with tearing-parity structures**.

2. These modes saturate by modifying and relaxing the edge current sheet

$\gamma\tau_{A(n=1)} = 0.16,$
$\gamma\tau_{A(n=2)} = 0.18,$
$\gamma\tau_{A(n=3)} = 0.2,$
$\gamma\tau_{A(n=4)} = 0.23,$
$\gamma\tau_{A(n=5)} = 0.26.$
$S = 2 \times 10^5$

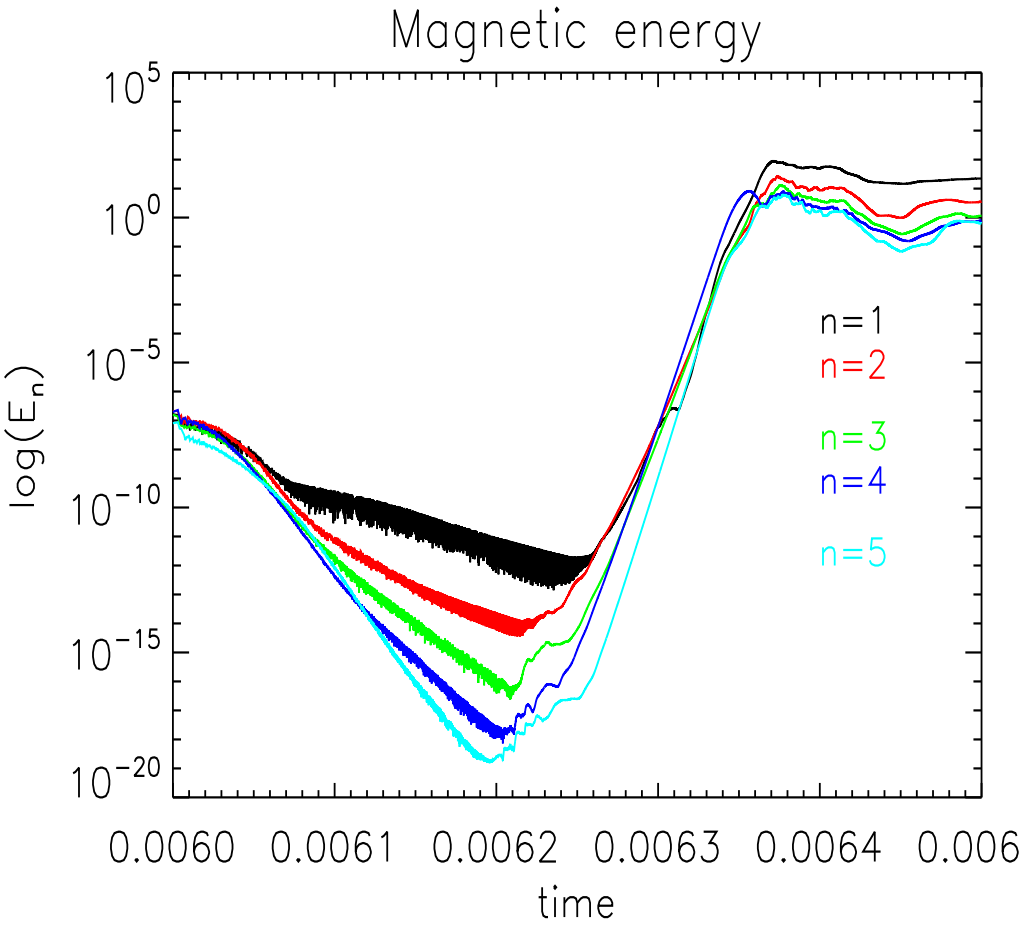

PPPL PRINCETON UNIVERSITY

Poloidal flux amplification is observed to trigger axisymmetric reconnecting plasmoids formation

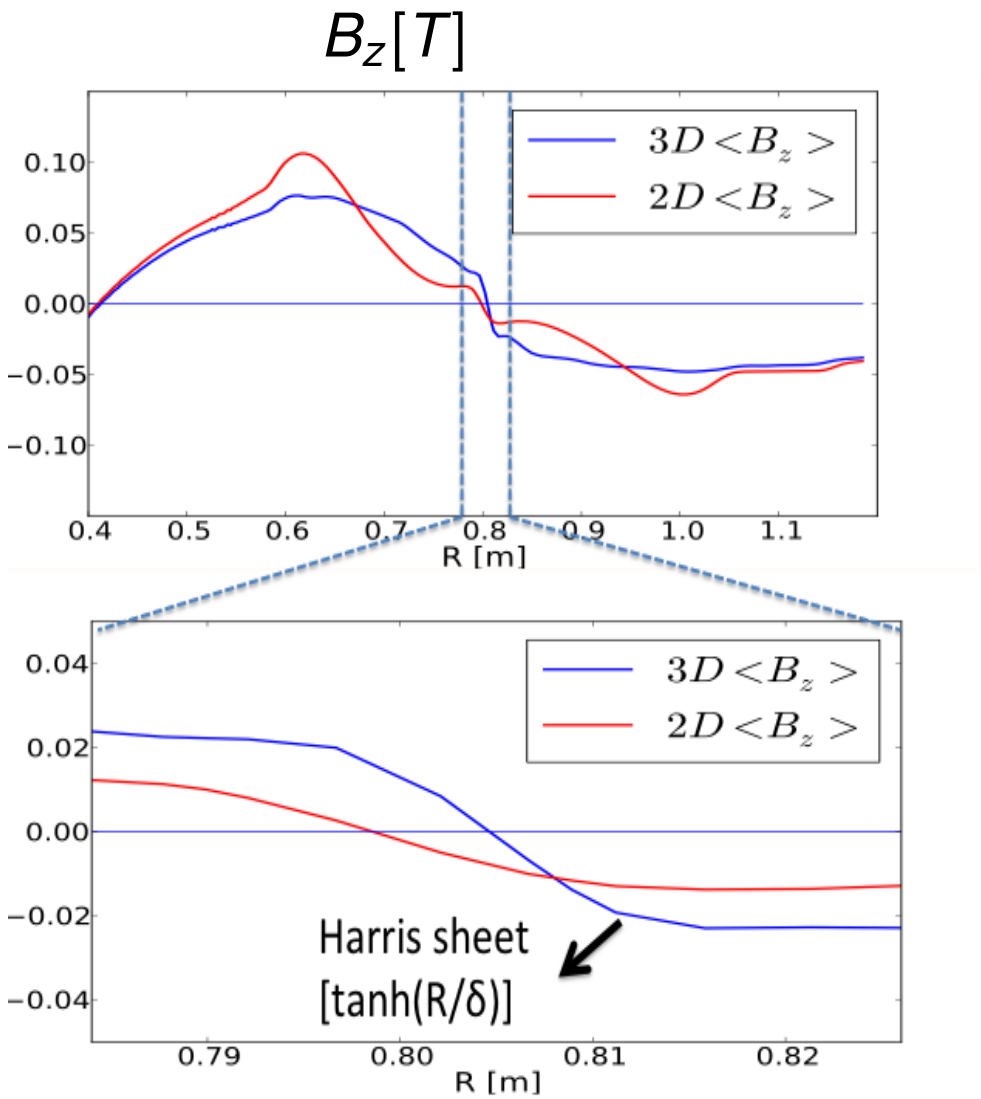

- For the first time a dynamo poloidal flux amplification is observed
- This **fluctuation-induced flux amplification increases the local S**
  ==>
  triggers a plasmoid instability
  ==> breaks the primary current sheet.

PPPL PRINCETON UNIVERSITY

Observational evidence of plasmoid-like structures

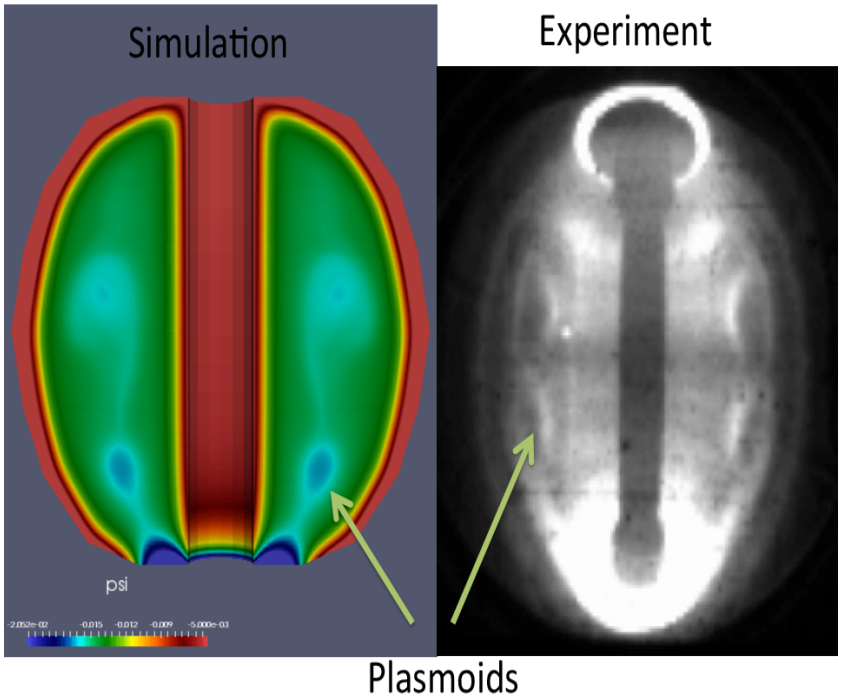

Camera images from NSTX do show the formation, and subsequent separation, of smaller plasmoids that then merge into a larger pre-existing plasma.[Ebrahimi&Raman PRL 2015]

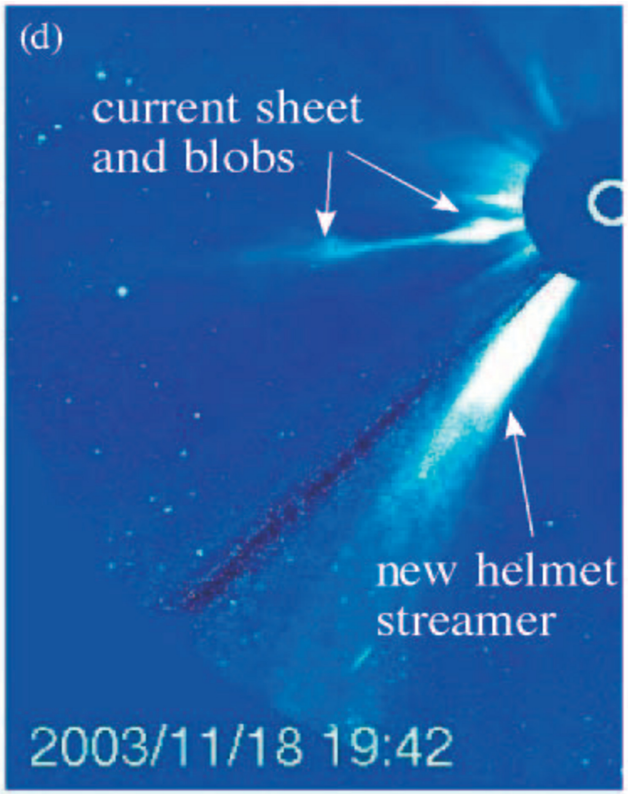

Plasmoids (2D) of the reconnected plasma flowing along the current sheet.LASCO/SOHO C3 images [Lin et al. 2005; Reily et al. 2007]

PPPL PRINCETON UNIVERSITY